PACIFIC EARTHQUAKE ENGINEERING RESEARCH CENTER

Rocking Response of Bridges on Shallow Foundations

José A. Ugalde
University of California, Davis
Staff Engineer
Fugro West, Inc.

Bruce L. Kutter
Boris Jeremić
University of California, Davis

PEER 2010/101
APRIL 2010

Technical Report Documentation Page

1. Report No. PEER 2010/101	2. Government Accession No.	3. Recipient's Catalog No.
4. Title and Subtitle Rocking Response of Bridges on Shallow Foundations		5. Report Date April 2010
		6. Performing Organization Code
7. Author(s) José A. Ugalde, Bruce L. Kutter, and Boris Jeremić		8. Performing Organization Report No.
9. Performing Organization Name and Address Center for Geotechnical Modeling Department of Civil and Environmental Engineering University of California, Davis, CA, 95616		10. Work Unit No. (TRAIS)
		11. Contract or Grant No.
12. Sponsoring Agency Name and Address California Department of Transportation Sacramento, CA 95814		13. Type of Report and Period Covered Final Report
		14. Sponsoring Agency Code

15. Supplementary Notes

This report covers results and findings from Project: STAP13 — Design Guidelines for Foundation Rocking of Bridge Piers.

16. Abstract

The goal of this research is to address concerns about the suitability of using rocking shallow foundations for bridges. The research quantifies how combined moment, shear and axial loading affect behavior rocking behavior and illustrates the beneficial energy dissipation and self-centering characteristics that shallow foundations can introduce to the system. Due largely to these self-centering characteristics, rocking foundations appear to be quite resistant to instability as a result of P-Δ effects.

Even if design guidelines were made to allow for rocking and the design philosophy included using shallow foundations as a mechanical fuse limiting structure loads, allowing soil to yield under a shallow foundation and mobilization of the moment capacity of the footing will not be used unless there is an accurate method of analysis. For this reason, existing elements and analysis tools available in OpenSees were exercised to show that they can reasonably predict the behavior of rocking foundation systems.

Several centrifuge tests were carried out at UC Davis on models of single-column bridge bents on shallow foundations. The experimental data from these tests along with the experiments done by many researchers (Gajan et al. 2005; Taylor et al. 1981; and Faccioli et al. 2001; and others) on the load-displacement behavior of shallow foundations and soil-structure interaction shed light on the rocking behavior of a shallow foundation and its influence on a bridge superstructure. The experimental data were then used to exercise and verify finite element tools for a range of structures on rocking foundations.

17. Key Word Bridge Piers, Spread footings, Rocking, Uplift, Shaking Table Tests, Centrifuge tests, Computer modeling, Earthquake Response, Design Guidelines	18. Distribution Statement No restrictions. This document is available through the National Technical Information Service, Springfield, Virginia 22161

19. Security Classif. (of this report) Unclassified	20. Security Classif. (of this page) Unclassified	21. No. of Pages 86	22. Price

Form DOT F 1700.7 (8-72) Reproduction of completed page authorized

Rocking Response of Bridges on Shallow Foundations

José A. Ugalde
Graduate Student Researcher
Department of Civil and Environmental Engineering
University of California, Davis
Staff Engineer
Fugro West, Inc.
Oakland, California

Bruce L. Kutter and Boris Jeremić
Department of Civil and Environmental Engineering
University of California, Davis

Prepared under Award Number 59A0433 (STAP13)
in cooperation with the
State of California
Business, Transportation, and Housing Agency
Department of Transportation

PEER Report 2010/101
Pacific Earthquake Engineering Research Center
College of Engineering
University of California, Berkeley

April 2010

ABSTRACT

The goal of this research is to address concerns about the suitability of using rocking shallow foundations for bridges. The research quantifies how combined moment, and shear, and axial loading affect behavior rocking behavior and illustrates the beneficial energy dissipation and self-centering characteristics that shallow foundations can introduce to the system. Due largely to these self-centering characteristics, rocking foundations appear to be quite resistant to instability as a result of P-Δ effects.

Even if design guidelines were made to allow for rocking and the design philosophy included using shallow foundations as a mechanical fuse limiting structure loads, allowing soil to yield under a shallow foundation and mobilization of the moment capacity of the footing will not be used unless there is an accurate method of analysis. For this reason, existing elements and analysis tools available in OpenSees were exercised to show that they can reasonably predict the behavior of rocking foundation systems.

Several centrifuge tests were carried out at UC Davis on models of single-column bridge bents on shallow foundations. The experimental data from these tests along with the experiments done by many researchers (Gajan et al. 2005; Taylor et al. 1981; and Faccioli et al. 2001; and others) on the load-displacement behavior of shallow foundations and soil-structure interaction shed light on the rocking behavior of a shallow foundation and its influence on a bridge superstructure. The experimental data were then used to exercise and verify finite element tools for a range of structures on rocking foundations.

ACKNOWLEDGMENTS

This research was funded primarily by the State of California Department of Transportation (Caltrans) under award number 59A0433 entitled STAP13: Design Guidelines for Foundation Rocking of Bridge Piers. This work was also supported in part by the Earthquake Engineering Research Centers Program of the National Science Foundation under award number EEC-9701568 through the Pacific Earthquake Engineering Research Center (PEER) project number 1412006. Publication of this report was funded by the PEER Transportation Systems Research Program. Any opinions, findings, conclusions, or recommendations expressed in this material are those of the authors and do not necessarily reflect those of the funding agencies.

The authors gratefully acknowledge Caltrans Project Managers Craig Whitten and Fadel Alameddine, who provided invaluable advice and leadership throughout the project.

The present work was based upon previous work performed by Sivapalan Gajan, who provided advice and guidance throughout the project. Sashi Kunnath also provided guidance and suggestions during the course of this work. This project was performed in close collaboration with Stephen Mahin and Andres Espinoza, structural engineers at the University of California, Berkeley. The close collaboration between geotechnical and structural engineers was a key to the project's success. Our discussions on bridge design and physical modeling were very helpful in focusing this research toward practical applications. The staff at the Center for Geotechnical Modeling, especially Dan Wilson and Chad Justice, were instrumental in the successful completion of the centrifuge experiments carried out as part of this research.

DISCLAIMER

The contents of this report reflect the views of the authors who are responsible for the facts and accuracy of the data presented herein. The contents do not necessarily reflect the official views or policies of the State of California. This report does not constitute a standard, specification, or regulation.

CONTENTS

LIST OF FIGURES

LIST OF TABLES

1 Introduction

1.1 MOTIVATION

According to the Caltrans Technical Report *Bridge Retrofit Construction Techniques*, “Footing work tends to be the most difficult and costly of all retrofit measures. It should be avoided at all costs.” The three options discussed for shallow foundation retrofitting in this document are adding piles and tie downs, and increasing footing dimensions with multiple references to creating resistance to uplift of the footing.

The statements in the document summarized above are part of the motivation behind the research of the rocking behavior of bridges on shallow foundations. First, foundation work is expensive. Second, the retrofit decisions are limited to fixing the foundation and preventing uplift which, in fact, has been observed to be beneficial to structures during earthquakes (Housner 1963).

Other than retrofit decisions, engineers need to make decisions when constructing new bridges. For seismic design, the seismic design criteria (SDC v1.4 2006) and numerous memos to designers (MTD) are available. The seismic design philosophy is described in the MTD 20-1. Understandably there should be a pre-determined location of damage which can easily be inspected and repaired after an earthquake. MTD 20-1 indicates that the preferred locations for inelastic behavior are the columns, pier walls, back walls, wingwalls, seismic isolation and damping devices, bearings, shear keys, and steel end-diaphragms. There is no mention of designing for inelastic behavior of the soil under a shallow foundation.

This leads to the other motivation behind this research besides the question of use of rocking as a way to decrease retrofit costs and improve seismic performance, which is design philosophy. The current design philosophy is based on the ductility capacity of structural members. It ignores the soil yielding under a shallow foundation as a ductile member even though it exhibits the characteristics desired in designed ductile failure members.

Although nonstructural members are not explicitly mentioned in the seismic design philosophy of MTD 20-1, it seems that the SDC recognizes the effect of foundation flexibility and takes it into account when calculating ductility demands in the structure. For new construction the SDC requires that the foundation capacity must exceed demands and that the nominal capacity of the foundation must be large enough to ensure that a column reaches its capacity first. The foundation capacity referred to is the capacity of the structural elements of the foundation as well as the soil-foundation interface strengths; consequently, the mobilization of the moment capacity of a shallow foundation is not allowed. The absence of any formulas for shallow foundation design, no mention of shallow foundations in seismic design, and concentration on the design of pile foundations in the SDC discourages the use of shallow foundations when there is any potential for rocking.

1.2 GOAL OF RESEARCH

The goal of this research is to address the concerns over using shallow foundations and to try to quantify and understand the phenomenon controlling:

capacity (vertical, moment, shear load combinations)

tip over (dynamic)

instability (static, because of stiffness degradation and P-Δ effect)

energy dissipation

self-centering characteristics

and to then determine if the rocking of a shallow foundation is acceptable as a ductile component in design.

The last part of this research is to explore and exercise current analysis tools. Even if design guidelines were made to allow for rocking and the design philosophy included using shallow foundations as a mechanical fuse limiting structure loads, allowing soil to yield under a shallow foundation and mobilization of the moment capacity of the footing will not be used unless there is an accurate method of analysis. With the extreme importance of and focus on minimizing risk in engineering today, it is important to have a reliable way to predict behavior with reasonable precision. For this reason, accurate methods of analysis are necessary in order to account for foundation rocking in design.

In order to reach these research goals several centrifuge tests were carried out at UC Davis on model single-column bridge bents on shallow foundations. The experimental data from these tests along with the experiments done by many researchers (Gajan et al. 2005; Taylor et al. 1981; Faccioli et al. 2001; and others) on the load-displacement behavior of shallow foundations and soil-structure interaction (SSI) shed light on the rocking behavior of a shallow foundation and its influence on a bridge superstructure. This experimental data are then used to exercise and verify finite element tools for a range of structures for which the tools had not been previously verified.

1.3 PREVIOUS RESEARCH ON SHALLOW FOUNDATIONS: SYSTEMS, CONCEPTS, AND CONTROLLING PARAMETERS

1.3.1 Soil-Footing-Structure Rocking System

The rocking of a structure on shallow foundations is in most cases examined in one plane of motion. The three degrees of freedom associated with this plane of motion are vertical translation, horizontal translation, and rotation about the out-of-plane axis. Unless otherwise specified the notations used for the forces on the footing are those proposed by Butterfield et al. (1997). V is vertical load (positive downward), H is shear on the footing, and M is the moment on the footing about point O, as indicated in Figure 1.1.

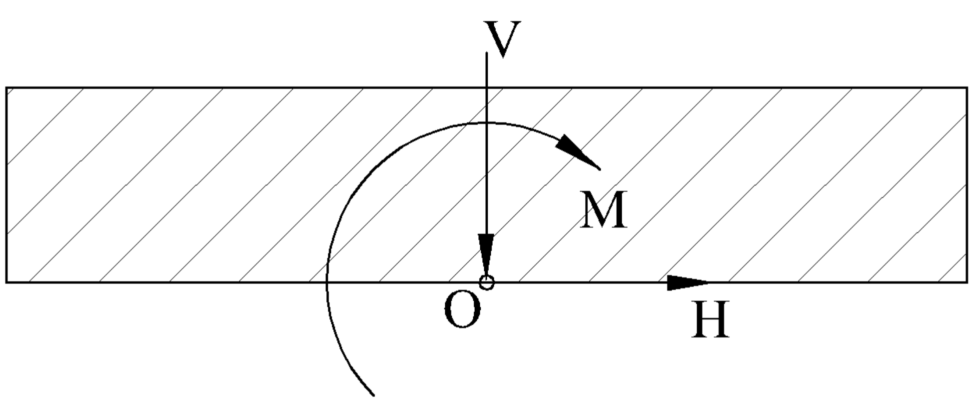

Fig. 1.1 Footing forces.

The soil-foundation-structure system examined in this report is a lollipop-like structure on a shallow spread footing. This model is used to simplify the typical single-column bridge bent. For the most part, motion is restricted to one plane in the modeling and analysis of this soil-structure system. The mass distribution is mainly in the footing and bridge deck with a typical footing mass of 15%–30% of the bridge deck mass. The footing and bridge deck are assumed to be rigid bodies, each with the three degrees of freedom described above.

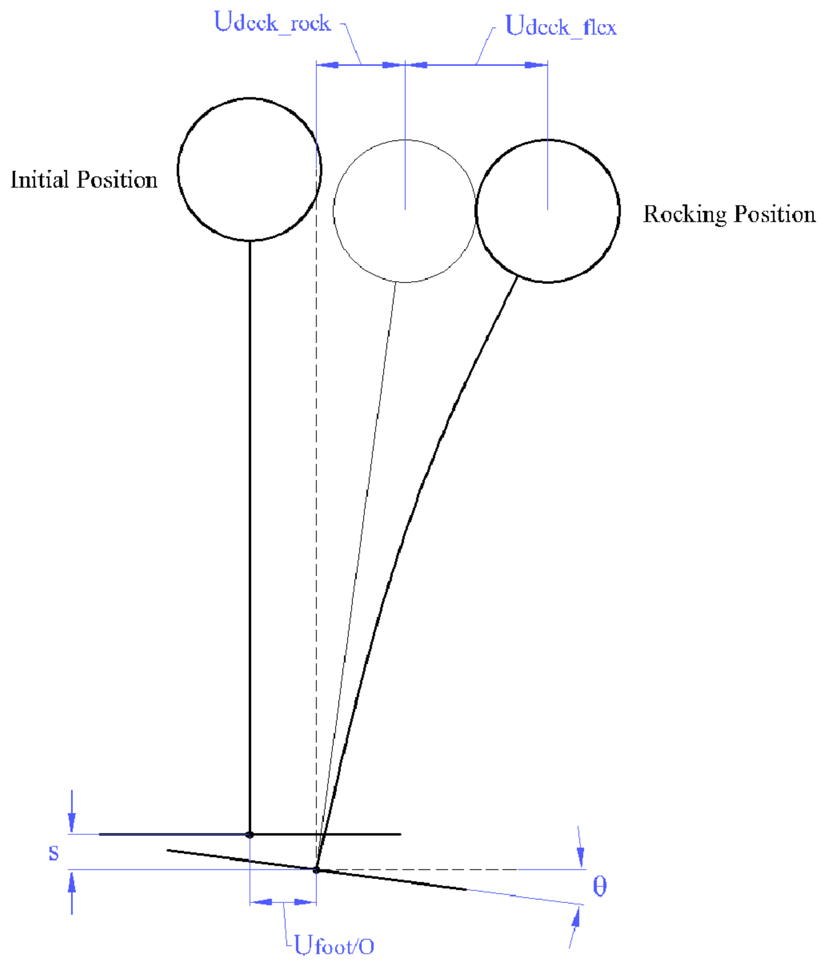

Fig. 1.2 Schematic of rocking system bridge system with displacements.

When the structure is loaded the foundation settles, slides, and rotates. As the foundation rotates, one corner will start to uplift, reducing the soil-footing contact length. As the soil-footing contact length decreases, the pressure under the footing increases as vertical equilibrium is satisfied. At some rotation the pressure under the portion of the footing in contact with soil reaches the ultimate bearing capacity (q_{ult}). Once the soil has reached its bearing capacity, the length of footing in contact with soil has reached what will be called the critical contact length

(L_C). The contact length cannot become smaller than L_C as long as the bearing capacity does not increase and the vertical load remains constant.

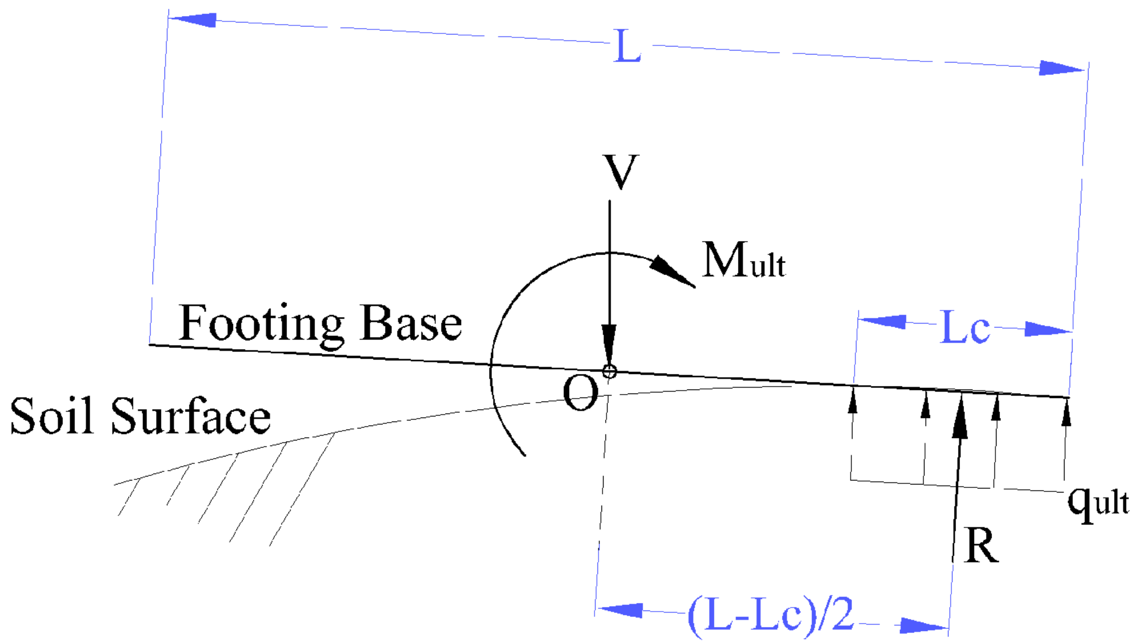

Fig. 1.3 L_C, L, rotating footing, forces, reaction, and pressure distribution.

1.3.2 Controlling Parameters

The response of a rocking shallow foundation is affected by both material and geometric nonlinearities. The material nonlinearity will be controlled by the soil failing under L_C. This in turn dictates how the soil surface is rounded during rocking that controls the geometric nonlinearities. So, the geometry affects the yielding which in turn affects the geometry. This interaction between geometric and material nonlinearity, in addition to the nonlinear behavior of structural components, makes the characterization of the global nonlinear behavior difficult to understand. The most important parameters controlling the load-deformation behavior of a shallow foundation (for the case of lateral loading with constant vertical load) have been found to be the vertical load (V), the critical contact length (L_C), the length of the footing in the plane of rocking (L), and the ratio of moment to shear on the footing (Gajan 2006).

1.3.3 Load Capacities

It is assumed in the following formulations that the pressure distributions under the soil-footing contact area are constant. Many researchers have shown that the actual shape of the pressure distribution has a small effect on the calculated capacities. Under pure moment and vertical loading the capacity can be calculated by summing moments about point O in Figure 1.3 and by assuming that the resultant soil reaction R is equal to V for small rotations.

$$M_{cap} = \frac{V}{2} \cdot \left(L - L_c \right) \tag{1.1a}$$

Factoring out L from the second term in Equation (1.1a),

$$M_{cap} = \frac{V \cdot L}{2} \cdot \left(1 - \frac{L_c}{L} \right) \tag{1.1b}$$

The ratio L_C/L is shown by Gajan et al. (2005, 2006) to control the capacity (Eq. 1.1), the energy dissipated in the soil under the footing during earthquakes, and the dynamic and permanent displacements of the footing. In many cases the ratio L_C/L is written as q/q_{ult} or $1/FS_V$, where FS_V is the vertical factor of safety on bearing capacity. The fact that L_C is a function of the dimensions of the footing-soil contact area is often ignored. The approximation of

$$\frac{L_c}{L} = \frac{q_{fullcontact}}{qult_{Mcap}\left(L_c, B_c, c', \varphi', \gamma, D_f\right)} \approx \frac{q_{fullcontact}}{qult_{Vcap}\left(L, B, c', \varphi', \gamma, D_f\right)} = \frac{1}{FS_V} \tag{1.2}$$

where

L_C = Critical contact length: Length of footing in contact with soil when moment capacity is mobilized

B_C = Critical contact width: Width of footing in contact with soil when moment capacity is mobilized

c', ϕ' = Soil strength parameters defining the failure envelope

γ = Effective unit weight of soil under footing

D_f = Depth of embedment of footing

$(q_{ult})_{Vcap}$ = Ultimate bearing capacity under pure vertical loading

$(q_{ult})_{Mcap}$ = Ultimate bearing capacity under vertical and moment loading is commonly accepted because the iterative procedure necessary for calculating L_C gives a false sense of accuracy given the uncertainty associated with calculating q_{ult} and the different bearing capacity factors, shape factors, and depth factors possible to use in the general bearing capacity equation. As FS_V increases, the approximation of $(q_{ult})_{Vcap}$ equal to $(q_{ult})_{Mcap}$ becomes less accurate as the size and shape of the contact area change dramatically during rocking; however, as FS_V increases M_{cap} becomes more of a function of the vertical load and the footing length. For example, whether L_C/L is 1/15 or 1/30, the calculated M_{cap} using Equation 1.1 will differ by only 3%.

Equation 1.1 shows the interaction between vertical load and moment capacity assuming no shear; however, the moment capacity does depend on the shear as well as the vertical load. Figure 1.4 shows a failure surface proposed by Houlsby et al. (2002) coupling the moment capacity to the vertical and shear loads. Coupled V-H-M failure surfaces have also been proposed by other researchers for both "cohesive" and "cohesionless" soil. One of the first of these types of failure surfaces was proposed by Georgiadis and Butterfield (1988) and verified by 1g tests on surface footings under different load combinations on sand.

The interaction between moment and shear capacities becomes important when the ratio of moment to shear is not large. It is convenient to use dimensionless quantities to describe the interaction so the ratio of moment to shear is normalized by the length of the footing. Although convenient, normalizing by the footing length does not remove all bias in the capacity interaction. Experiments by Gajan, Rosebrook, and Kutter show that for the same ratio of M/HL, increasing foundation embedment will increase the moment capacity closer to the theoretical capacity in Equation 1.1. Also, Gajan (2007) shows that for the ratio of M/HL above about 1.7, the effect of shear on moment capacity is negligible.

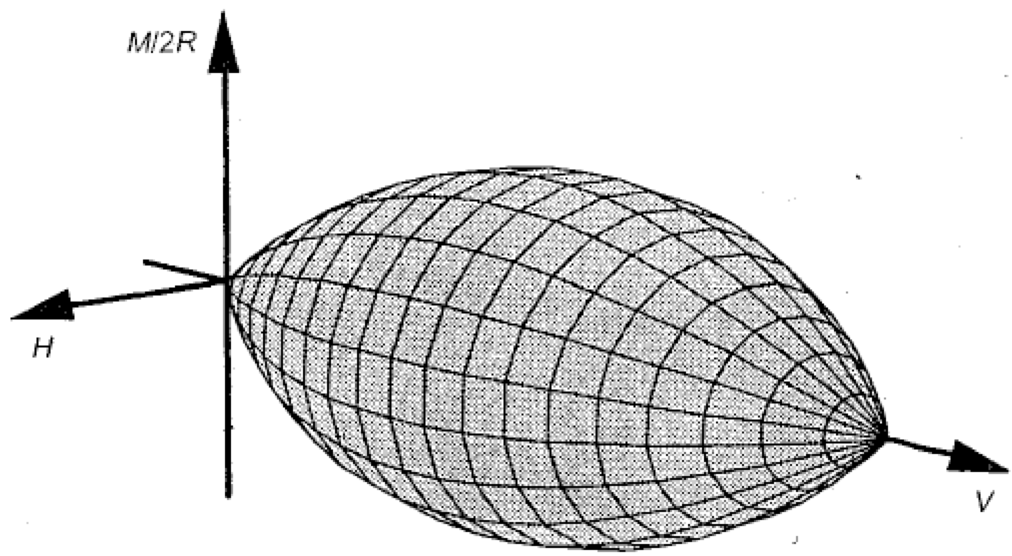

Fig. 1.4 Load capacity surface proposed by Houlsby and Cassidy (2002).

1.3.4 Energy Dissipation

Energy dissipated by rocking foundations was formulated by Housner (1963) for rigid blocks on a rigid half space. The assumptions used in this mathematical formulation are valid in many instances where energy is dissipated by radiation damping on an elastic base. If the base is elastic, the only way energy can be dissipated in the rocking mechanism is through radiation damping as assumed by Housner in his formulation and formulated in design procedures by Priestley et al. (1996). However, foundation uplift increases bearing pressures and commonly loads the soil well into the nonlinear range. The material hysteresis becomes a significant portion of the energy dissipation. Similar to the radiation damping formulation by Housner, material damping in the soil increases with the amplitude of displacement (settlement, sliding, or rotation). The hysteretic energy dissipated in the soil by foundation rocking can be summarized in the following equation:

$$dW = V \cdot ds + H \cdot dU_{foot/O} + M \cdot d\theta \tag{1.3}$$

For the typical bridge structure, most of the energy is dissipated in moment-rotation hysteresis. However, it is important to note that the V-ds and H-dU terms in Equation 1.3 cannot always be ignored. The main factor affecting the ratio of the energy-dissipation terms is the normalized moment to shear ratio (M/HL) (Gajan 2006). As this ratio decreases, the sliding mode participates more, which leads to more shear-sliding hysteresis (Fig. 1.5).

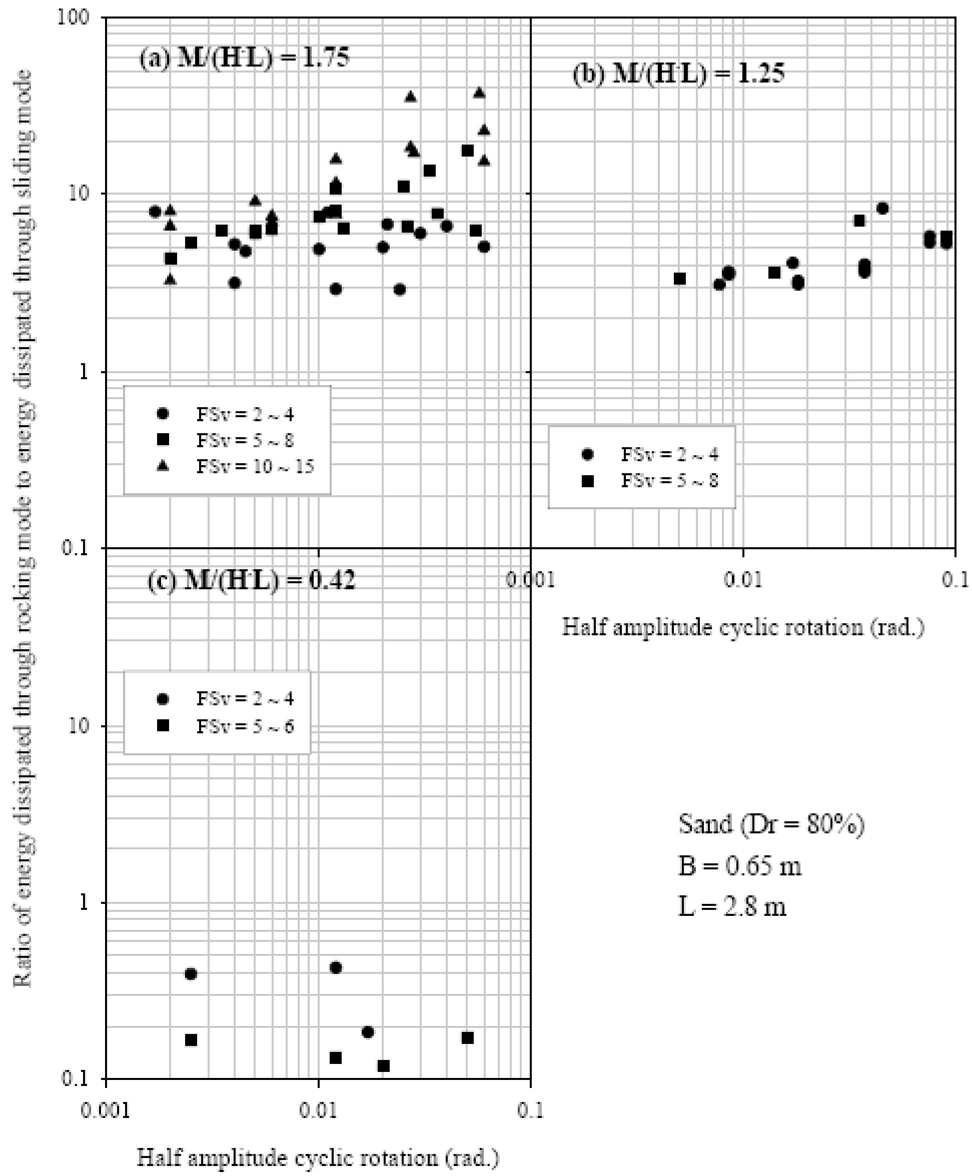

Fig. 1.5 Effect of FSV and M/(HL) ratio on the ratio of energy dissipation through rocking mode to sliding mode in lateral cyclic tests: (a) M/(H·L) = 1.75, (b) M/(H·L) = 1.24, (c) M/(H·L) = 0.42 (Gajan 2006).

A comparison of different energy-dissipation curves for rocking rigid blocks is shown in Figures 1.6a–b. The first set of figures show both measured energy dissipation per cycle and energy-dissipation ratio (EDR) from centrifuge experiments by Gajan et al. on rocking shear walls that were rigid relative to the foundation flexibility. EDR is defined by Gajan (2006) as:

$$EDR = \frac{Area\_of\_hysteresis\_loop}{4 \cdot (M\_\max\_cycl) \cdot (\theta\_\max\_cycle)} \tag{1.4a}$$

where M_max_cycle is the peak moment for the given cycle and θ_max_cycle is the footing rotation corresponding to the peak moment for that cycle. EDR turns out to be proportional to the equivalent viscous damping term defined by Chopra (2001).

$$EDR = \frac{\pi}{2} \cdot \zeta_{eq} \approx 1.57 \cdot \zeta_{eq} \tag{1.4b}$$

Figure 1.6b is based on the procedures in Priestley et al. (1996). The third comparison is to the design procedures used by Caltrans engineers and consultants (Alameddine et al. (2002), which assumes that a 10% damped spectrum leads to 30% reduction in spectral values from a 5% damped spectrum.

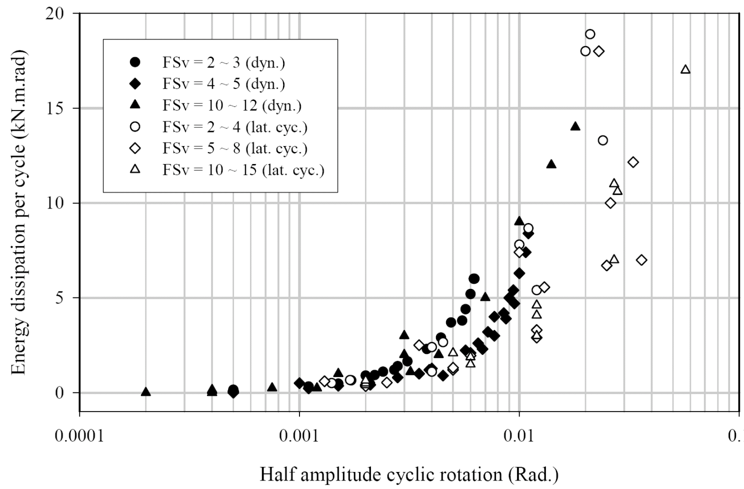

Fig. 4.52 Energy dissipation through foundation rocking versus amplitude of rotation for lateral cyclic (M/(H·L) = 1.75) and dynamic tests (Hcg/L = 1.8) with different FS_V range

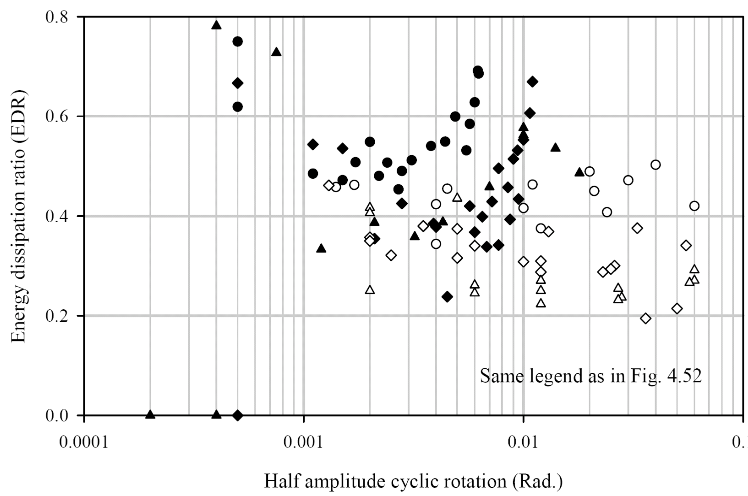

Fig. 4.53 Ratio of energy dissipation through foundation rocking versus amplitude of rotation for lateral cyclic (M/(H·L) = 1.75) and dynamic tests (Hcg/L = 1.8) with different FS_V range

Fig. 1.6 (a) EDR for rocking of rigid blocks based on centrifuge tests (from Gajan 2006) and (b) EDR for average structure in Fig. 1.6a (from Priestley et al. 1996) based on radiation damping on elastic half space (after procedures from Priestley et al. 1996).

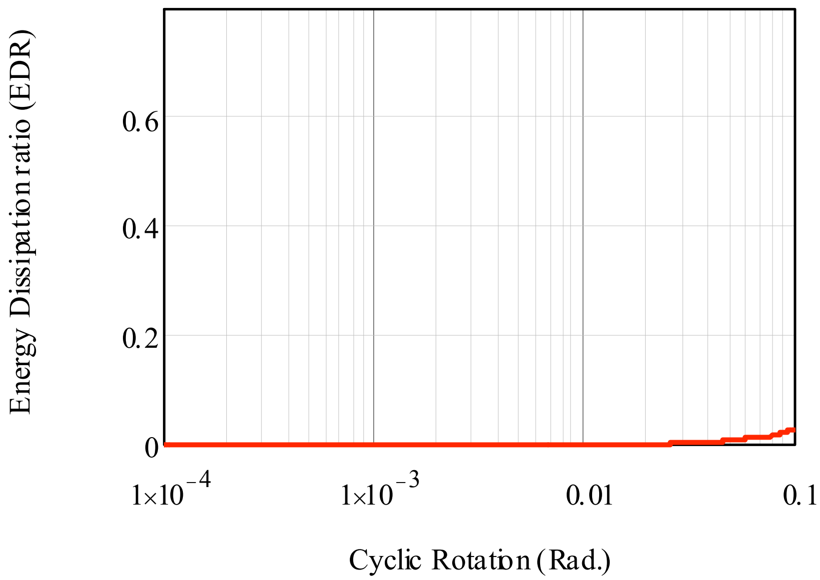

(b)

Fig. 1.6—*Continued.*

It is clear from Figures 1.6a–b that the assumption of the foundation as a rigid body on an elastic half space with only radiation damping is not valid in the case of shallow foundations rocking on soil because the predicted energy dissipated by radiation damping is an order of magnitude less than the measured values from centrifuge experiments. Also, using 10% damping across the board for foundation rocking will likely lead to unrealistic results, as the damping will be greatly underestimated. The rocking response is greatly determined by the energy dissipated in soil hysteresis, which is not included in the procedures proposed by Priestley. Hysteretic energy dissipation is a function of displacement amplitudes, which during a typical earthquake can lead to damping ratios of up to 50% (EDR of 80%), whereas radiation damping is frequency dependent. The contrast in stiffness between the soil and a rocking structure is not usually as favorable to radiation damping as hysteretic damping in the soil. The dominance of material damping has been shown in similar amounts of energy dissipated in pseudo-static and dynamic loading of structures on shallow foundations by Gajan (2006).

Aside from the amplitude of rotation the factor of safety on bearing capacity also affects the energy-dissipation ratio. Numerical modeling by Hu (2006) shows that the damping ratio and EDR of a rocking footing decreases as the factor of safety on bearing capacity increases.

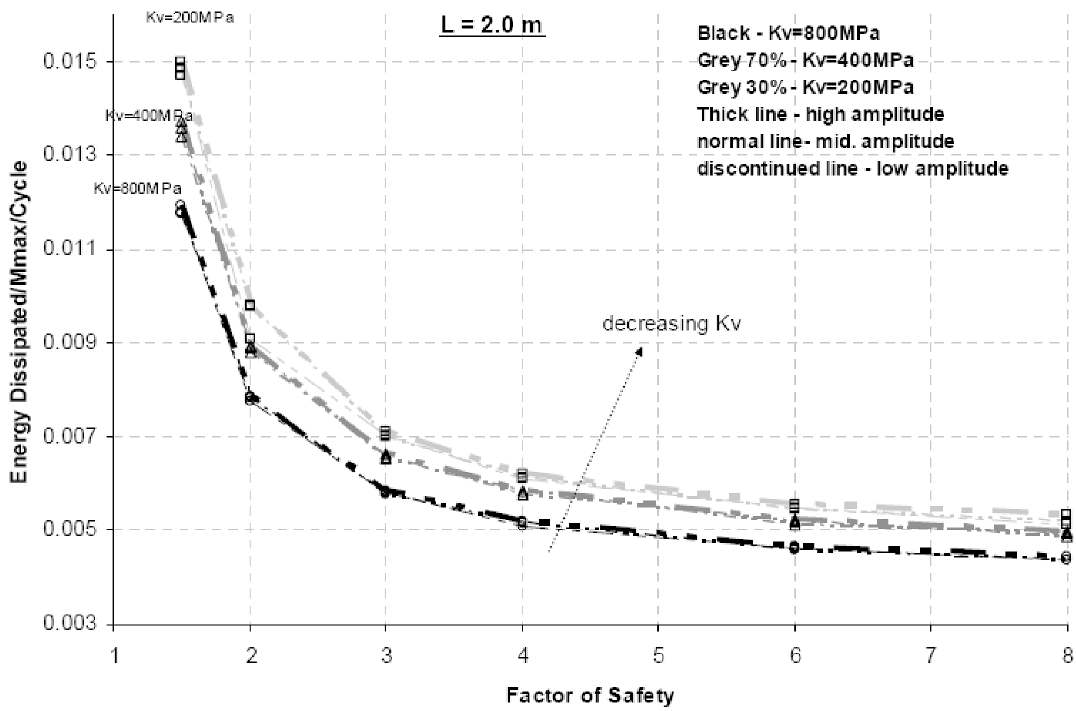

Fig. 1.7 Effect of factor of safety on the normalized energy dissipated under a rocking shallow foundation (after Hu 2006).

1.3.5 Structure Displacements

In the end, the single most important response characteristic that a design engineer cares to know is that the displacements of the superstructure are within some allowable range. This is dictated partly by the dynamic behavior of the structure and partly by the behavior of the foundation (Fig. 1.2). When motion is restricted to one plane both the deck mass and the footing which is typically 15–30% of the deck mass have three degrees of freedom. Depending on

the mass distribution,

the stiffness, the capacity, and the damping of each mode

and the loading scenario

the contribution of each of these modes can vary. Although under general loading any of these modes can be significant, in the analysis of rocking bridges under earthquake loading, the rotation of the footing and horizontal displacement of the bridge deck typically have been the only two modes considered in the rocking analysis of bridges.

In general, the dynamic behavior of bridges on shallow foundations has been analyzed from the structural engineer's perspective, while the general load-deformation behavior of shallow foundations has been studied extensively by geotechnical engineers.

Gajan (2006) described in detail the effect of the vertical factor of safety on bearing capacity (FS_V), moment to shear ratio (M/HL), depth of embedment, soil type, footing geometry, and unsymmetrical loading on load capacities, energy dissipation, and footing displacements under both pseudo-static and dynamic loading. From the geotechnical engineer's perspective many of the important parameters and their effects on displacements are summarized in Figure 1.8.

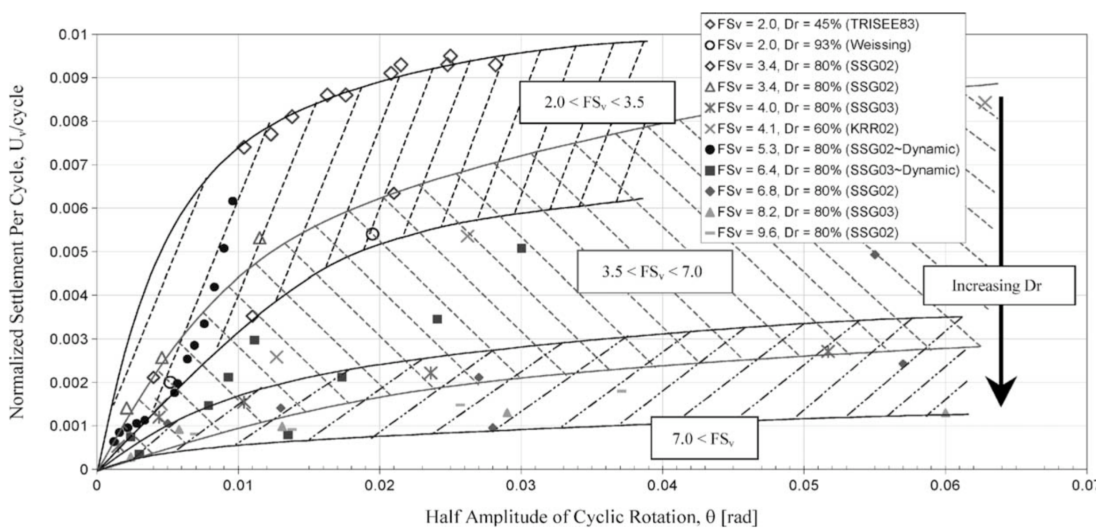

Fig. 1.8 Permanent settlement caused by cyclic rotation: slow cyclic and dynamic test results on sand for various FS_V and Dr (for height of push ~ 4-5m). (After Gajan 2006).

Although it is difficult to overstate the importance of the load-deformation behavior of the foundation on the overall bridge response, the assumptions of the behavior of the foundation made in analytical, numerical, or experimental models by different researchers all vary significantly.

Some examples of common approximations for modeling of a rocking bridge are

The soil is modeled as

a rigid half space with radiation damping on impact (Housner, Priestley, Zhang and Makris, WinROCK, others),

a bed of pressure-independent elastic springs (only geometric nonlinearities) (Mergos and Kawashima 2005), a bed of pressure-independent elastic perfectly plastic springs (geometric and material nonlinearities) (Mergos and Kawashima (2005)),

rubber (Espinoza et al., Sakellaraki et al. (2005)).

The foundation is modeled as free to

rotate,

rotate and translate,

rotate and settle, and

rotate, translate, and settle.

The results from all of these experiments with various modeling techniques and boundary conditions mostly show that allowing the foundation to rock reduces moment demands in the column and increases horizontal displacement demands on the bridge deck. The extent to which rocking reduces the moment demand depends on both the ratio of the horizontal stiffness and the capacity of the column to rotational stiffness, and the capacity of the foundation, damping, and the input motion. It is also important to note that allowing the foundation to rock does not guarantee reduced moment demands or increased displacement demands in all cases. If the rate of energy dissipation increases significantly as displacements increase, or the predominant input motion frequency is larger than the rocking fixed-base fundamental frequency of the structure, the opposite may be true.

Mergos and Kawashima (2005) examine the effects of uniaxial, biaxial, and triaxial excitation on a bridge on a square shallow foundation of varying size (Fig. 1.9). The model includes a constant bearing capacity and a 3-D Winkler foundation of elastic perfectly-plastic springs. They found that multi-axial excitation reduces moment demands in the column but increases deck displacements. This same trend is seen as the foundation size decreases.

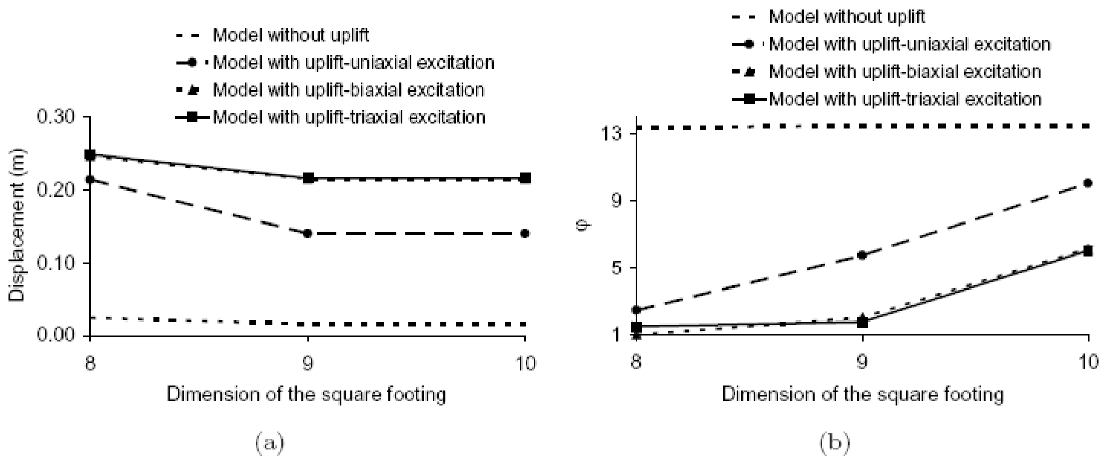

Fig. 1.9 Influence of size of footing on response of bridge: (a) Maximum deck displacements due to foundation rocking; (b) maximum curvature ductility demands at base of pier. (After Mergos and Kawashima 2005).

2 Centrifuge Experiments on Rocking Bridge Foundations

2.1 INTRODUCTION

A substantial amount of research has been conducted on the load-deformation behavior of shallow foundations and on the SSI of rigid bodies on soil and flexible structures on rubber, including numerical simulations of many of these systems. However, prior to the centrifuge tests described in this report, there have been no experiments on large flexible bridge structures that typically have large factors of safety with respect to bearing capacity. Some aspects modeled that are in combination unique to the JAU01 test series are:

- Relatively large structure with a flexible column;
- Large ratio of center of gravity/footing width (M/hL);
- Large contact pressures and large factors of safety comparable to typical bridge footing; many previous experiments were on smaller footings applicable to buildings;
- Soil used under the model footing (not rubber or other flexible soil substitutes);
- Dynamic earthquake ground motions applied to some structures;
- Slow controlled cyclic footing loading applied to some structures;
- Multiple shaking events;
- Square footing geometries; and
- Realistic footing boundaries without restriction of out-of-plane movements.

The scope and the important procedures of the centrifuge test will be described herein, although more details about the test setup and procedures can be found in the centrifuge data report for JAU01 (Ugalde et al. 2008).

2.2 CENTRIFUGE MODELING PRINCIPLES

As described by Schofield (1980), Kutter (1995), and Wood, scaling factors for centrifuge modeling are well established in the literature. The basic centrifuge scaling laws can be derived by defining the length scale factor as $L^* = L_m/L_p$ by assuming that identical materials are used in the model and the prototype (hence material densities scale according to $\rho^* = \rho_m/\rho_p = 1$), and by requiring that the stresses in the model should scale to be identical to those in the prototype; i.e., $\sigma^* = \sigma_m/\sigma_p = 1$. Because soil has nonlinear mechanical properties that are a function of confining stress, it is important that stresses scale one to one. Simple dimensional analysis shows that $\sigma^* = 1$ may be accomplished by increasing accelerations (including gravity) by a factor $a^* = 1/L^*$ and scaling time by $t^* = L^*$. For the JAU01 test series experiments discussed in this report, $L^* = 1/42.9$ and $a^* = 42.9$.

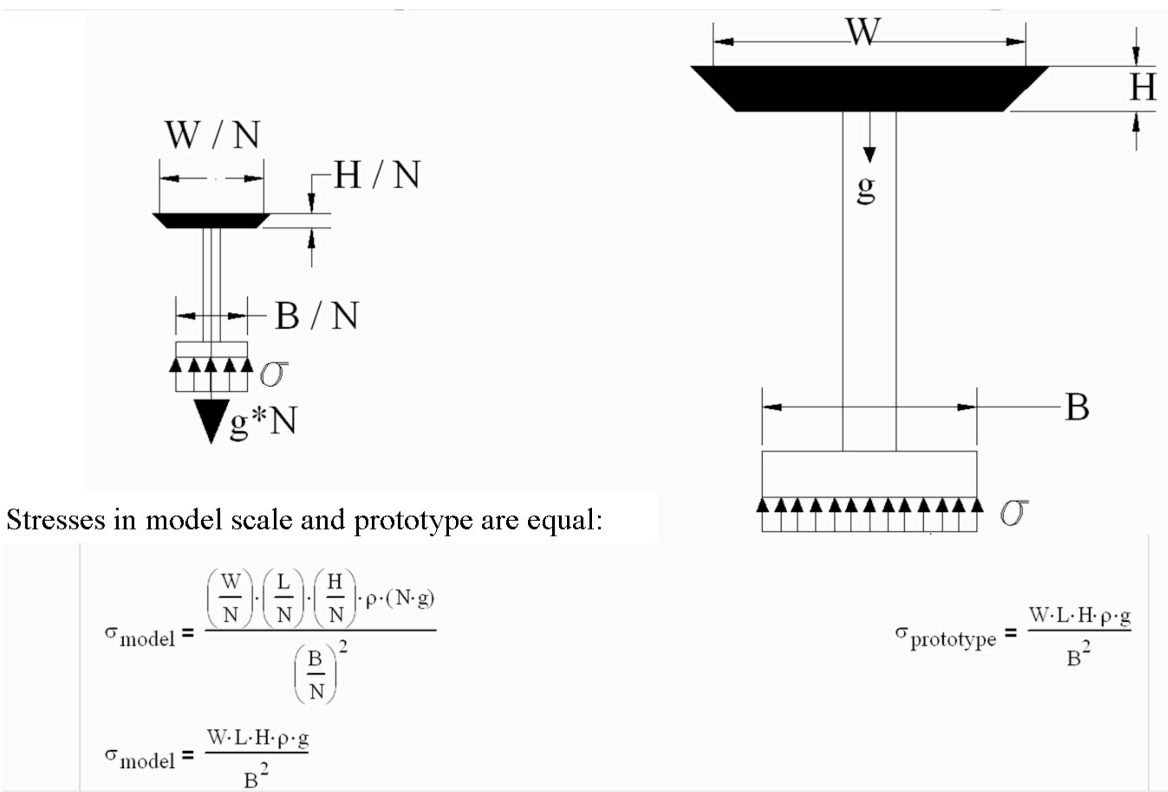

Fig. 2.1 Centrifuge scaling laws.

It is important to note that while stress scales properly, soil plastification and ultimately failure, usually characterized by development of shear bands, do not scale. This is because the length scale of the failure zone (shear band) is usually 5–20 soil particles, which, if the same soil is used in the prototype and model scales, does not scale. This lack of scaling might have implications for the observed mechanical behavior and especially for energy dissipation in the model scale, which will not be possible to scale up to that of the prototype. This lack of scaling of the failure zone needs to be further investigated.

2.3 JAU01 TEST PROGRAM

JAU01 was the first test series undertaken to understand the rocking behavior of bridges on shallow foundations under nonlinear moment, shear, and vertical loading. The test is part of a collaborative project with UC Berkeley, including 1-g shake table testing, in order to recommend improved design guidelines for bridges on shallow foundations. Both rigid and flexible structures were placed on a dense sand foundation. The rigid structures were used in pseudo-static cyclic horizontal push tests in order to carefully explore the cyclic load-deformation behavior of different sized shallow foundations. These pseudo-static tests are referred to as "slow-cyclic" tests in figures and text, consistent with the terminology used by Gajan et al. Flexible "lollipop" structures consisting of aluminum columns and steel masses representing the bridge deck were used to model the dynamic response of single-column bents on shallow foundations subject to earthquake loading.

Testing was performed on many test structures that were placed at different stations in a large soil container. The structures were spaced so that they were an adequate distance from each other and the walls of the container. Each structure location was given a station name, Station A through Station G. Slow cyclic tests at Stations A and B were directly loaded with a hydraulic actuator and Stations C through G (Figs. 2.2 and 2.3) were excited by ground motions applied to the base of the soil container.

The model tests were scaled from typical bridge configurations used by Caltrans. The prototype footings were square with widths of 3, 4, or 5 times the diameter of the column (Dc =1.8 m). The prototype scale mass and width of the footings at dynamic stations C, D, E, and F are (336 Mg, 8.9 m), (246 Mg, 7.1 m), (173 Mg, 5.4 m), and (246 Mg, 7.1 m), respectively. The mass of the deck at stations C, D, E, and F is 926 Mg. The fixed-base natural period of these structures is 1.6 sec. The total structure mass and footing width of structures at stations A and B are (1250 Mg, 8.9m) and (1080 Mg, 5.4m) respectively. Nevada Sand (mean grain size of 0.15 mm) was placed by dry pluviation in air to a uniform relative density of about 80% to create a 210 mm deep soil deposit in the 1.76 x 0.9 m (75.6 x 38.9 m prototype scale) model container.

For this density, and for pressures appropriate to the footing loads, the friction angle is about 40°–42° (Gajan 2006). The foundation soil contained accelerometers for measuring both vertical and horizontal accelerations.

The vertical bearing capacity of a shallow foundation on sand for bridge structures turns out to be quite large (F = 17 to 50 for the experiments described here). This large factor of safety with respect to bearing capacity is reasonable because the governing criteria for large footings on sand tend to be the allowable settlement and the required moment capacity; bearing capacity does not determine their size. The footings are sized by allowable bearing pressures. The footings described herein had bearing pressures that ranged between 80% and 150% of the pressure that would be expected to cause 25 mm of settlement under the static vertical loads.

The prototype structure was a typical reinforced concrete (RC) single-column bridge bent modeled as a "lollipop" structure with a deck mass and column connected to a shallow spread footing. Figures 2.2 and 2.3 depict the system modeled in the centrifuge tests carried out at UC Davis. The deck was modeled by a steel block; the reinforced concrete column was modeled by an aluminum tube that had a bending stiffness EI closely scaled to the calculated EI of the cracked section of the prototype concrete column. The footings were constructed of aluminum plates with sand glued to their bases to provide a rough concrete-like interface with the soil.

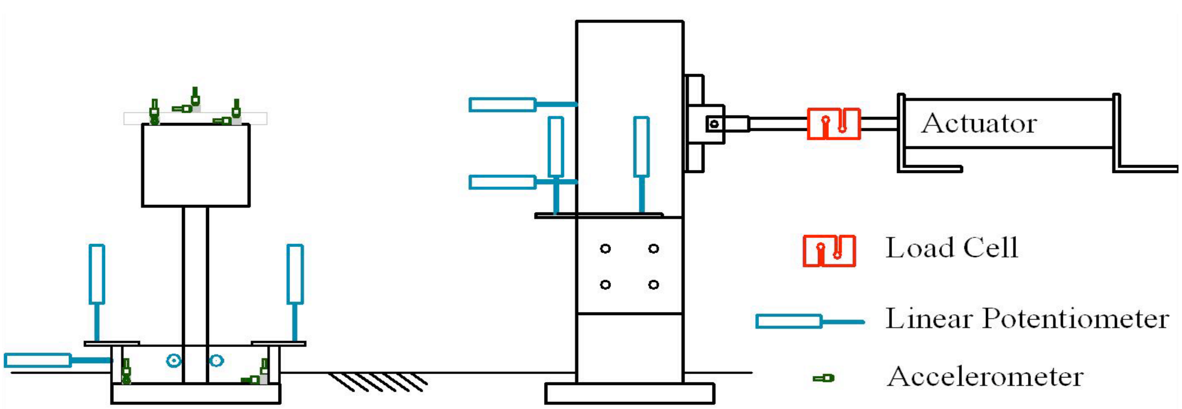

Fig. 2.2 Side view of structures and instrumentation for dynamic test and slow cyclic test.

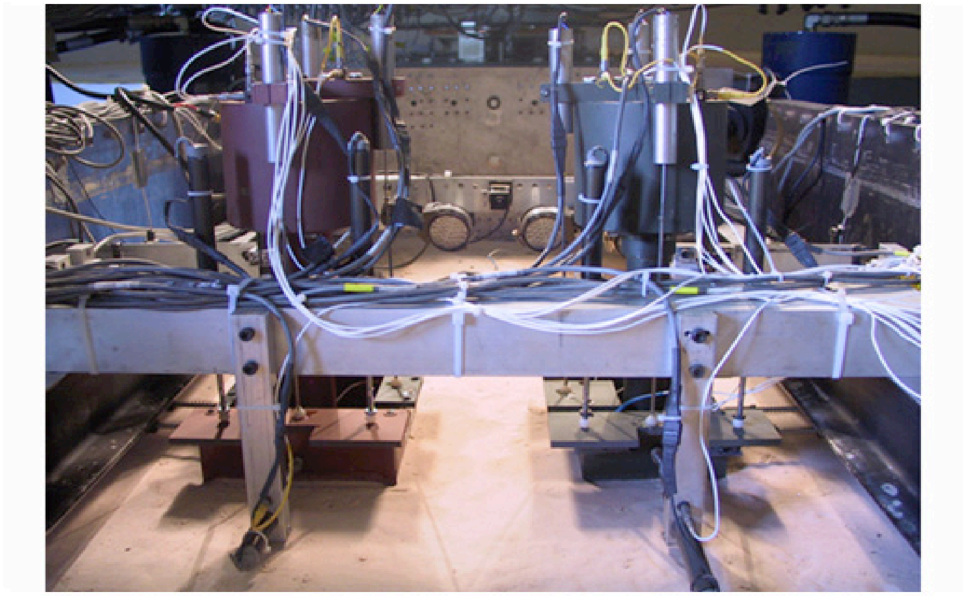

(a)

(b)

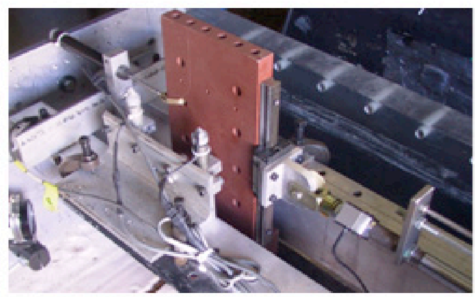

(c)

Fig. 2.3 (a) Two dynamic stations fully instrumented. (b) Gapping around perimeter of footing after slow cyclic test. (c) Connection between top of rigid wall with bearing rail attachment to load cell and actuator in a slow cyclic test.

For slow cyclic tests, the vertical load on the footing was scaled, but the distribution of the mass and the stiffness of the structure were not considered important parameters. Therefore, essentially rigid steel plates were used to provide the desired mass, and the wall acted as a vertical cantilever upon which lateral loads were applied by a hydraulic actuator acting horizontally at a height approximately equal to the elevation of the effective height of center of gravity of the prototype deck-footing system.

2.4 LOADING AND TEST SETUP SEQUENCE

At the time that the sand was placed, all seven model foundations were embedded to a depth of 40 mm (1.7 m prototype) at seven stations (A–G). Structures at one or two stations were tested during a given spin; the structures were bolted to their embedded foundation, then the centrifuge was spun and the loading events were applied. After stopping the centrifuge, the model structures were removed and new structure(s) were placed at other station(s) for testing in the next spin.

The sequence of testing involved 5 different spins. Prior to the first spin, a rigid wall structure was attached to the square footing. Then an actuator was attached to the wall as depicted in Figure 2.2. Teflon buttons against the sides of the wall provided the small lateral load necessary to prevent out-of-plane movement as described in detail by Gajan (2006). After spinning up to 42.9 g, slow cyclic lateral loading was applied by an actuator. The actuator was typically commanded to apply packets of 3 cycles of a sinusoidal displacement wave. For Stations A and B, 8 to 12 packets of sine waves with amplitudes varying between 0.14% to 5.4% of the effective height were applied to the structure.

Structures at Stations C–G were subject to dynamic loading using the shaking table mounted on the centrifuge to shake the entire model container. The ground motions imposed on the model container were scaled and filtered motions from recordings from the Tabas 1978 earthquake and a Los Gatos recording of the 1989 Loma Prieta earthquake. These motions come from the near-field records posted at the SAC Steel Project (2006) website. Twelve to fifteen scaled motions were applied to each structure. The testing sequence for dynamic stations started with low-amplitude step waves, followed by scaled-down earthquake ground motions, then large amplitude earthquake ground motions and finally step waves similar to those applied before strong shaking. The peak ground accelerations ranged between 0.1 g and 0.8 g.

The instrumentation is depicted in the drawings in Figure 2.2 as well as in the photos in Figure 2.3. For slow cyclic testing, each structure was instrumented with a load cell to measure the horizontal actuator load and four displacement transducers; any three of the four displacement sensors was sufficient to determine the rotation, settlement, and sliding of the footing.

2.5 DATA PROCESSING PROCEDURES

The acceleration and displacement data were acquired using the data acquisition infrastructure available at the center for geotechnical modeling. More details on the data acquisition infrastructure are available at:

https://central.nees.org/?facid=276&equipid=294&action=EquipmentList.

LabView was used to acquire the data, which were then processed in Mathcad.

The procedure for processing the data for all tests begins with windowing the acquired data set to capture some time before the loading event took place and some time after loading had finished. The data in the original binary data file are windowed, and then exported as a text file.

After windowing the original data files, the data were converted to prototype units using the centrifuge scaling laws described in Section 2.2, the gain factor to account for the amplification of the instrument signal, and the calibration factor that converts model-scale electronic units into prototype scale engineering units. Once in prototype units, displacements and accelerations were calculated using a combination of filtered scaled instrument readings. These procedures can be seen in the Mathcad data processing sheets and procedures in the JAU01 data report (Ugalde et al. 2008).

3 Experimental Results

3.1 INTRODUCTION

The model tests described herein and elsewhere have shown that the soil around the foundation does not remain elastic and that a significant amount of energy is dissipated by foundation rocking through moment-rotation, shear-sliding, and vertical load-settlement hysteresis (Gajan et al. 2005; Taylor et al. 1981; and Faccioli et al. 2001).

Some of the known effects of rocking are summarized below:

Peak moment demand in the column is limited by moment capacity of the foundation. In this respect the foundation can act like a mechanical fuse.

Uplift of a foundation stores gravitational potential energy. Closure of the gap upon unloading restores the footing toward its initial position.

Local bearing pressures increase causing plastic deformation of soil around the footing, which is a source of hysteretic damping.

Rocking results in lengthening of the natural period, which tends to reduce acceleration and force demands and increase displacement demands on the superstructure.

The magnitude of settlement caused by rocking depends on the number of cycles and amplitude of loading, as well as the bearing capacity.

One goal of this report is to help engineers to quantify the above factors so that rocking may be accounted for in the design process. If properly quantified, the benefits of rocking may be used to reduce construction costs without unduly sacrificing performance.

3.2 EXPERIMENTAL RESULTS

The definitions of displacements and forces on the footing and deck mass are more general than the terms used from Chapter 1 to describe rocking in one plane. In order to calculate forces and displacements of the centrifuge model structures in all six degrees of freedom the displacements in Figure 3.1 are used in calculating the structural load-deformation. The data from all of the accelerometers and displacement transducers mounted at various points on the foundation and the deck were combined and processed to provide the measurements of the translational and the rotational accelerations, and the displacements at the center of gravity of the foundation and the deck mass. The deck mass included attached instrumentation and half the column mass. The footing mass included the attached instrumentation, half of the column mass, as well as the plastic frame fixed to the foundation.

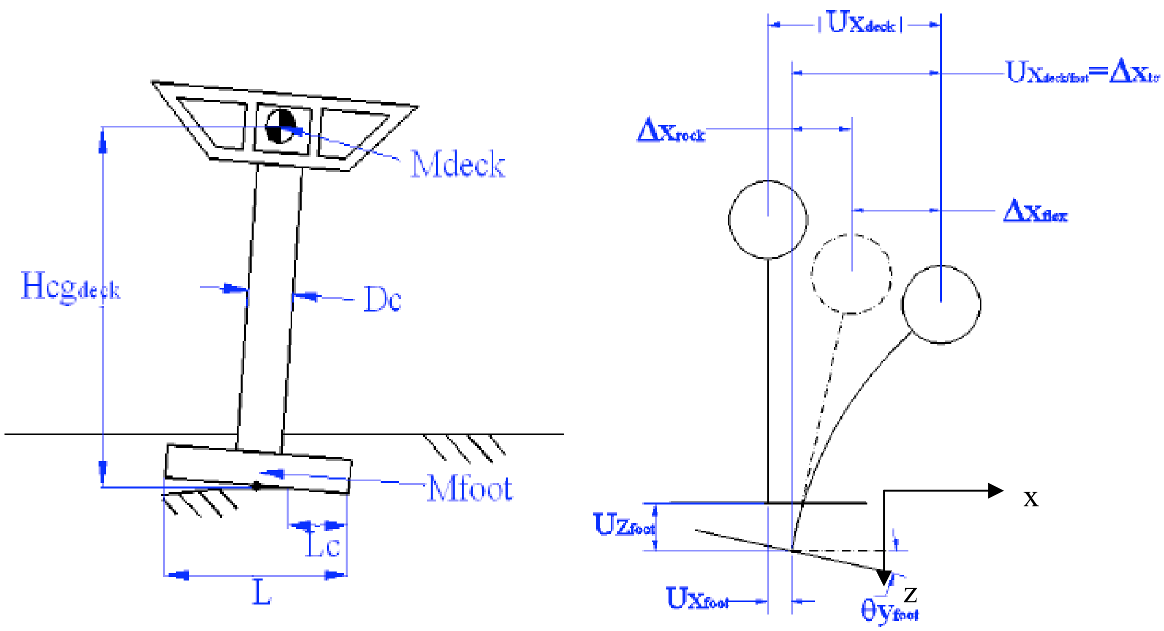

(a) (b)

Fig. 3.1 (a) Schematic of problem and definition of some system parameters. (b) Definition of coordinate system and displacements; x is horizontal in predominant plane of rocking and z is downward.

The rocking moment, M_y, and the horizontal sliding force, F_x ,computed at the base center point of the footing are calculated as follows:

$$M_y = (m * a_x * Hcg)_{deckcg} - (I * \alpha_y)_{deckcg} + (m * a_x * H_{cg})_{footingcg} - (I * \alpha_y)_{footingcg} + (m * (1g - a_z) * -U_{x_{deck/foot}})_{deckcg} \tag{3.1}$$

$$F_x = -(m * a_x)_{deckcg} - (m * a_x)_{footingcg} \tag{3.2}$$

The five terms in Equation (3.1) represent the moments due to lateral acceleration of the deck, the rotational acceleration of the deck, the lateral acceleration of the footing, the rotational acceleration of the footing, and the static and dynamic P-Δ moments. The greatest contributor to moment is the first term, the inertial force from the deck mass. At large rotations the P-Δ term becomes significant. The I*α terms of the deck mass and foundation are relatively small. But inclusion of these terms in the equation resulted in significantly improved data quality. Some "noise" that appeared in the data was eliminated by accounting for the moments due to the I*α terms. The inertial forces associated with added mass of the soil adjacent to the footing were neglected.

3.2.1 Slow Cyclic Tests

As seen in Figure 3.2, both the smallest (B = 3 Dc) and the largest (B = 5 Dc) foundations show large moment-rotation loops indicating significant energy dissipation. The moment capacity shows negligible degradation with the amplitude of rotation.

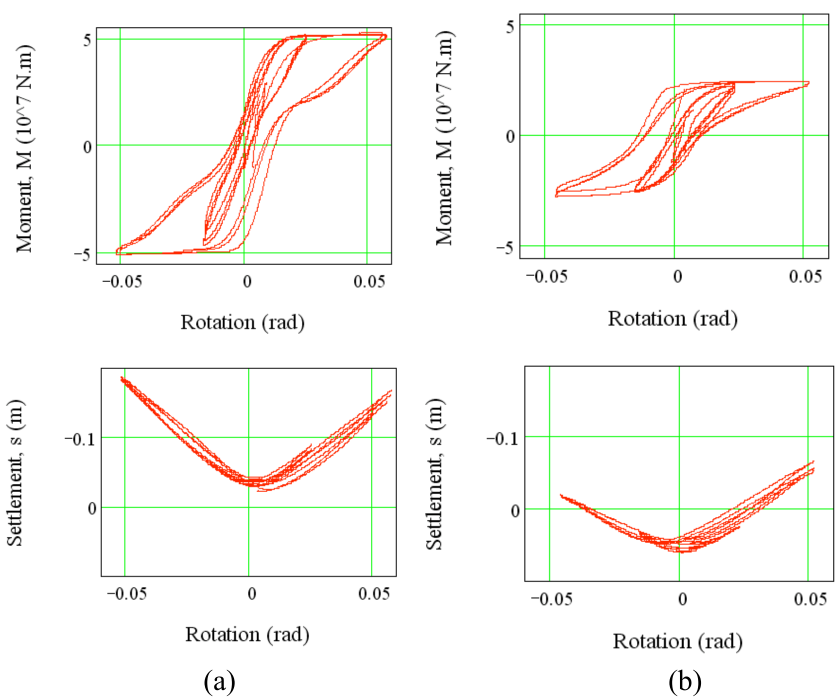

Fig. 3.2 Slow cyclic load-deformation behavior of footing (a) B = 3 Dc (b) B = 4. Dc.

The footings show mobilization of their moment capacity at about 2% rotation. The smaller footing (B = 3 Dc) has about 3/5 of the moment capacity of the largest footing (B = 5 Dc), consistent with expectations for rotation about one edge of the footing. The theoretical moment capacity (Eq. 1.1) for the case of a square footing may be expressed as:

$$M_{capacity} = V(B - B_C)/2 \tag{3.3}$$

Where V is the vertical load, B is the footing width, and B_c is the width of the footing required to support the vertical load V. The fact that the moment capacity for the small footing is slightly less than 3/5 of the capacity of the large footing is expected because the mass of the small footing is slightly less than that for the large footing (vertical load V is slightly smaller) and furthermore, for the small footing, B_c is a larger fraction of the total width, B.

The shape of the moment-rotation loops for the large foundation differs from that for the small foundation in that a larger percentage of the plastic rotation is recovered by the large foundation. Figure 3.2(a) shows a sudden recovery of rotation while unloading from about 2.5 to 1.5 x 10^7 Nm. The flag-shape-type hysteresis loop seen in the larger foundation is hypothesized to be caused by soil falling underneath the foundation during uplift. The gap around the edge of the footing, shown in Figure 2.3, appeared to develop by soil sloughing under the footing to fill gaps formed during rocking. For a given amplitude of rotation, the size of the gap is proportional to the footing size; because the gap is larger for a large footing, the sloughing of particles under the large footing may be more significant than it is for the small footing. Settlement rotation plots show that the larger foundation has a net uplift after the series of tests, while for the smaller footing, there is a net settlement. This is also consistent with the hypothesis that soil was falling into the gap under the large footing.

3.2.2 Dynamic Tests

Figure 3.3 shows the moment-rotation and the settlement-rotation response of the two structures simultaneously loaded during a scaled version of the Los Gatos ground motion. These structures are identical except for their foundation widths. During dynamic shaking both footings show a net settlement. The larger footing has a larger bearing capacity and smaller rotations. The shapes of the moment-rotation curves are similar to those observed in the slow cyclic tests shown in Figure 3.2.

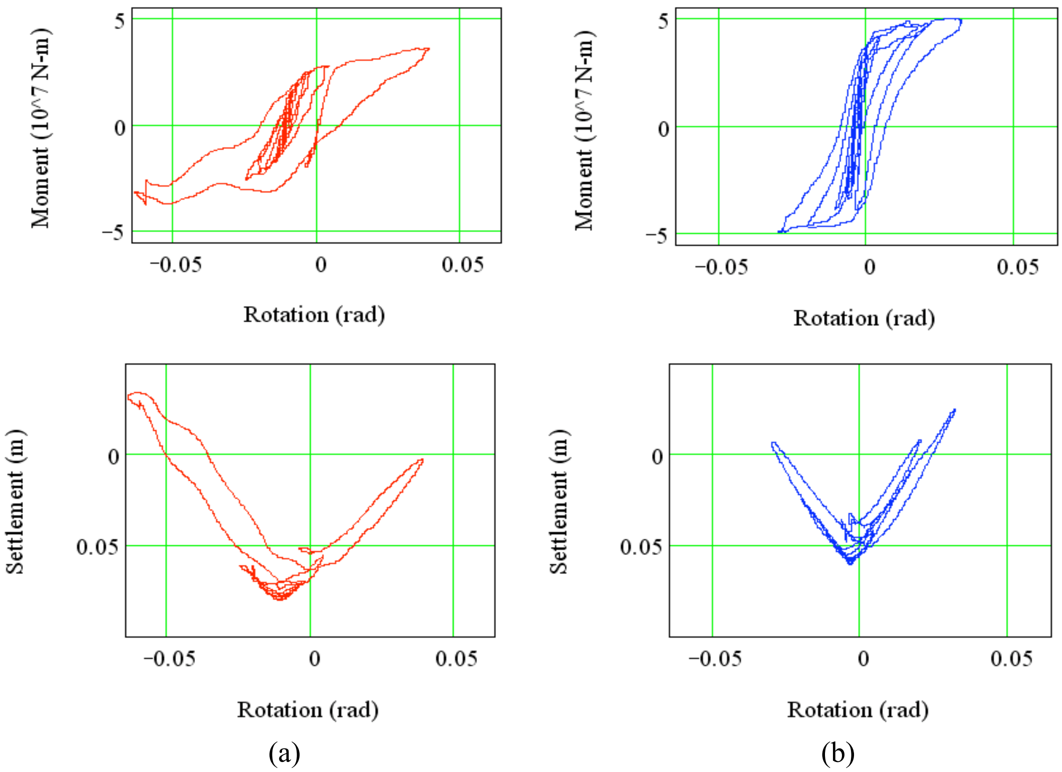

Fig. 3.3 Moment rotation and settlement rotation loops for Los Gatos event scaled to pga of 0.55 g . (a) Station E (B=3 Dc). (b) Station F (B=4 Dc).

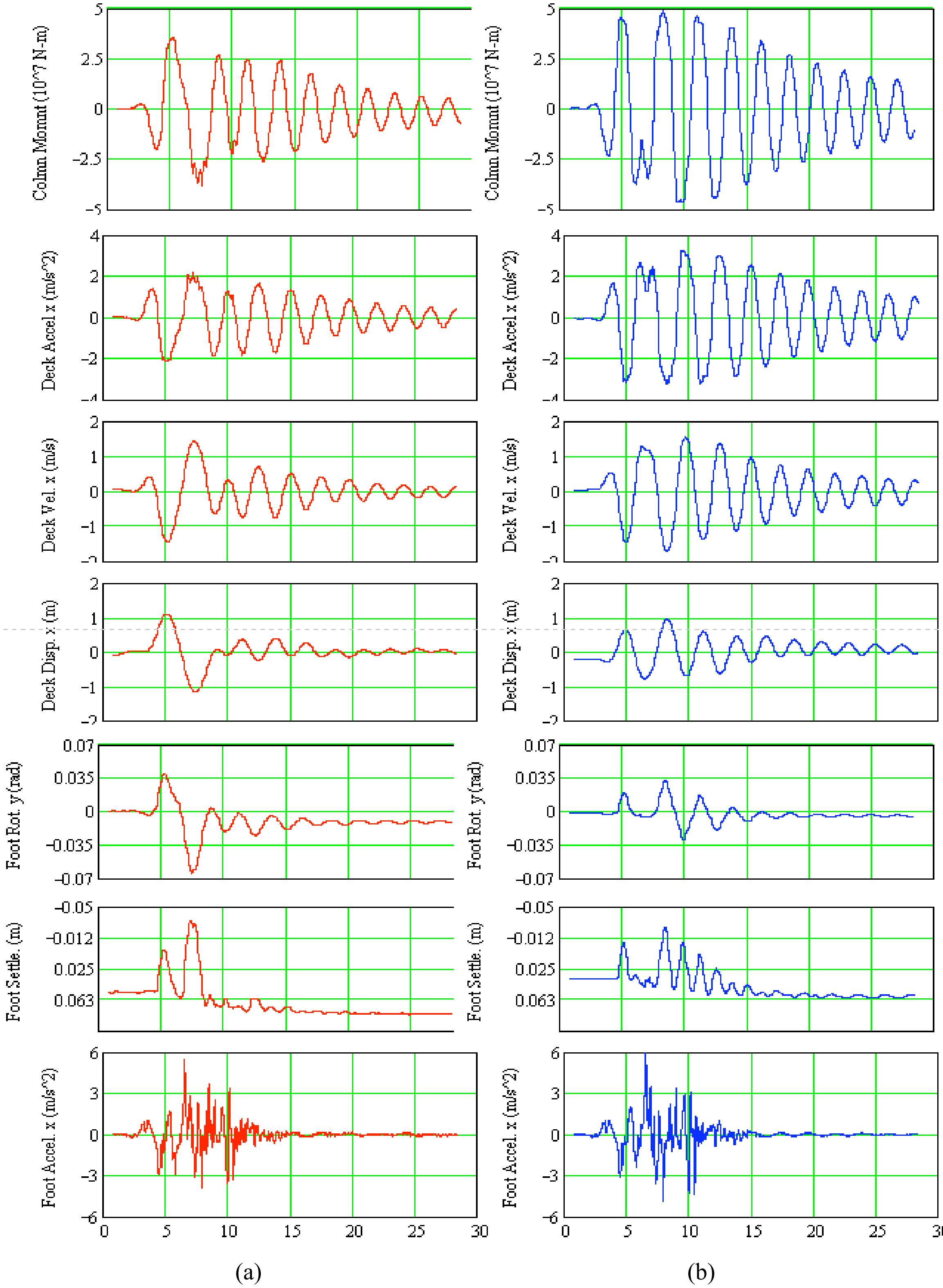

Fig. 3.4 Time histories for 0.55 g Los Gatos event. (a) (B = 3 Dc), (b) (B = 4 Dc).

Figure 3.4 shows the time histories of column moment, deck acceleration, velocity and displacement, and the footing rotation, settlement, and the horizontal acceleration for Stations E and F. The column moment time histories show that the structure with B = 3 Dc has about 20% smaller moment demand than the structure with B = 4 Dc. The acceleration along the shaking direction at the center of gravity of the deck mass is proportional to the largest term contributing to the moment (first term in Eq. 1). As such, it makes sense that the deck acceleration time history is very similar to the column moment time history. (The sign of the moment and acceleration time histories are opposite due to the sign convention.) The deck velocity for B = 3 Dc has only two large peaks, while that for B = 4 Dc has a slightly larger peak velocity followed by many large-amplitude velocity cycles.

The peak deck displacements for the small footings are approximately 15% higher than for the large footing. Larger displacement demands are expected for the small footing because the rotational stiffness of the foundation decreases as the footing width becomes smaller. It must be noted, however, that the dynamic response of a system depends upon the relationship between the system natural period and the predominant period of the shaking, and that the rocking natural period depends on footing size and the amplitude of the rocking. The footing rotation time histories show that the B = 3 Dc footing experienced two large-amplitude rotation pulses followed by many smaller cycles, while the B = 4 Dc footing has more cycles but of smaller amplitude. Both foundations experience approximately a 0.5% change in permanent rotation. A strong correlation is observed between footing rotation and settlement, indicating that most of the settlement is caused by moment and not by shear force or vertical loading. The settlement time history shows the position of the center of the base of the footing. Positive spikes correspond to uplift, which occurs at twice the frequency of rocking; an uplift cycle occurs when the foundation rocks to the right and another when the foundation rocks to the left. The last time series in Figure 3.4 shows the horizontal acceleration of the center of gravity of the foundation along the direction of shaking. The footing response is quite similar for both footings.

Figure 3.5(a) shows the acceleration response spectrum of the ground surface free field motion and the motion of the center of gravity of the deck mass for B = 3 Dc and B = 4 Dc during the 0.55 g Los Gatos event. Both rocking structures attenuate the short-period motions and amplify the long-period motions. Note that the fixed-base period of both structures is approximately 1.6 sec, and the natural period for the rocking systems (based on the deck accelerations in Fig. 3.5) was observed to be approximately 2.2–3 sec, depending on the amplitude of rocking.

The dynamic testing showed that as footing size decreased, the permanent deformations increased and the moment demand on the column decreased. The B = 3 Dc footing settled at about 30 mm per large shaking event while the structures on the larger foundations (B = 4 Dc or 5 Dc) settled at about 15 mm per strong shaking event.

Figure 3.5(b) shows the largest amplitude peak, the third largest amplitude peak, and the fifth largest amplitude peak column moments for a sequence of shaking events imposed on the structures with B = 3 Dc and B = 4 Dc, subject to the same shaking event. From this it is easily seen that during large shaking events, the capacity of the foundation limits the moment demand on the column. The peak column moments are consistently larger for the larger footing.

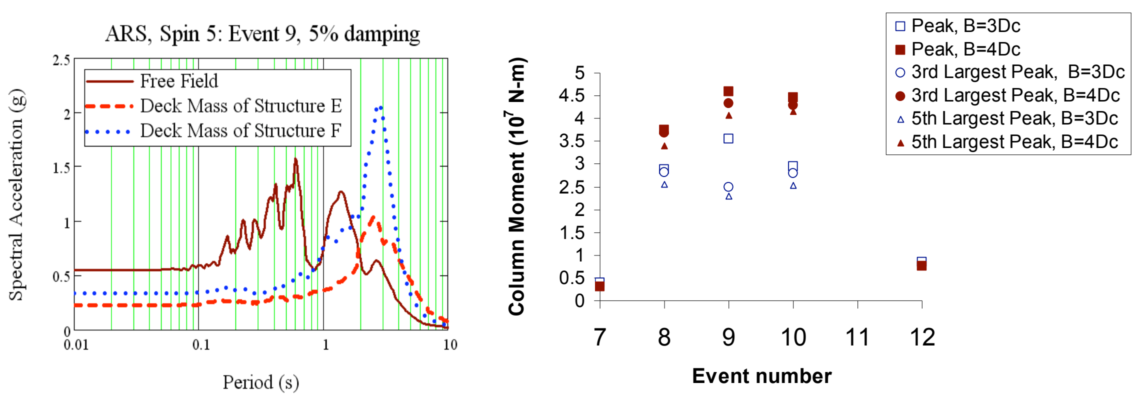

(a) (b)

Fig. 3.5 (a) Acceleration response spectra for ground surface motion and motions of the decks for Stations E and F during 0.55g Los Gatos motion (event 9). (b) Peak moments in column during the strong shaking events in Spin 5.

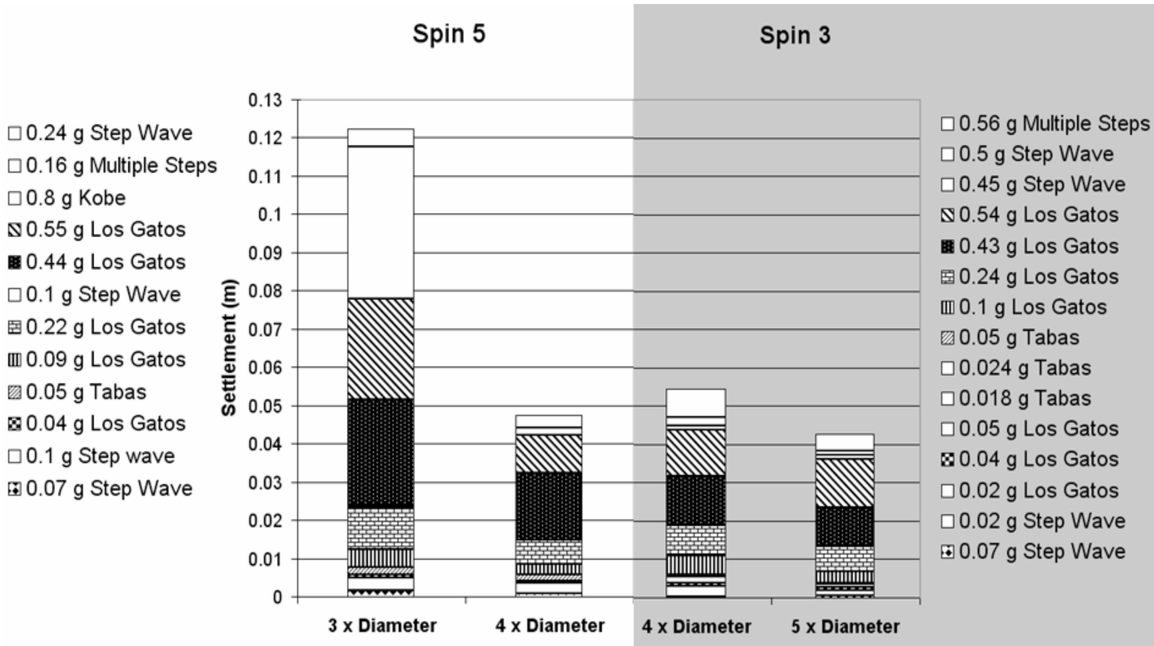

Fig. 3.6 Accumulated settlements for different foundation widths. Similar motions have same patterns.

3.3 DISCUSSION

3.3.1 Dynamic vs. Slow Cyclic Tests

There were some differences in the load-deformation behavior of the foundation under slow cyclic testing and dynamic testing. The amplitude of foundation rotations during dynamic testing tended to be smaller than those imposed during slow cyclic testing. The amplitude of rotation depends on the dynamics of the system and the frequency content of the ground motion; hence the amplitude of dynamic deck response also varied with footing size. Despite the fact that the amplitude of rotation tended to be smaller during the selected ground motions for dynamic tests, settlements were larger during dynamic loading than during slow cyclic loading. This was due partially to the settlement of the ground surface during shaking, but also may be associated with a reduction in bearing capacity caused by dynamic shaking of the soil combined with dynamic loading from the footing. In all cases, the magnitude of settlements was small enough that the performance may be judged to be satisfactory. For the smallest footing in the largest shaking event, the settlements were about 30 mm per shaking event.

3.3.2 Comparison to Data from Previous Tests on Building Shear Walls

Gajan et al. (2005) and others have previously reported data from rocking foundations for shear walls of buildings. The present tests used much of the same equipment that was used by Gajan et al. (2005). The foundations for the bridge structures, however, have a few important differences from the foundations tested by Gajan et al. (2005). First, Gajan et al. (2005) tested relatively rigid walls while the present foundations supported a deck mass attached to the footing by a flexible column.

The shear wall foundations tested by Gajan et al. (2005) had factors of safety with respect to bearing failure of the order of 2 to 15, while the bridge foundations had factors of safety with respect to bearing capacity between about 30 and 70. The size of the bridge foundations was governed by allowable settlement and moment capacity, which led to very large factors of safety with respect to vertical bearing capacity. The bridge foundations were square, while most of the shear wall tests were rectangular, with moment loading in the stiff direction. Due to the above differences, permanent settlements of the rocking bridge foundations on medium dense sand appears to be significantly less than the settlements of building foundations founded on similar soil.

3.3.3 Mechanisms for Yielding and Predicting Failure

In seismic resistant design of bridge structures, the designer ought to make a conscious decision regarding the capacity and demand that will be placed on various elements of the system. One design philosophy is to allow yielding but prevent collapse during extreme shaking events. If yielding is to be allowed, a decision should be made regarding which elements should yield and then that these elements are ductile and with the capacity to withstand drastic degradation. Structural engineers tend to recommend that the yielding occur in the column because they can control the ductility and capacity of the column with reinforcing bars and confining steel and because damage to a column can be easily inspected, and evaluated.

Civil engineers are trained that soil properties are heterogeneous and uncertain; hence they may develop the false impression that the moment capacity of a spread footing has a high uncertainty. On the contrary, with the exception of footings with low factors of safety with respect to bearing capacity, the moment capacity of a spread footing is largely controlled by the size of the footing and the vertical load on the footing. These key factors can be determined with good certainty, and hence the moment capacity can be accurately calculated by Equation (3.3). The present study (along with work of many previous researchers) shows that a rocking foundation has very ductile behavior with negligible loss of capacity. Rocking foundations also have significant damping capacity. The uplift of a shallow foundation provides a self-centering mechanism associated with gap closure upon unloading. This self-centering upon unloading is not a typical characteristic of yielding reinforced concrete columns.

Assuming that yielding does occur during a large seismic event, the reparability of the yielded element should also be considered. Damage to concrete may be argued to be more dangerous than damage to soil. Under extreme cyclic loading, damaged concrete columns are likely to crack, spall, and crumble. Soil is already an assembly of tiny pieces of broken rock that are difficult to break into even smaller pieces. Soils derive their strength from reliable friction as opposed to concrete cohesion that disappears upon cracking. Practical procedures such as grouting are available that could be used to close up the gaps and restore full contact between the footing and soil. Considering the above factors, yielding of a rocking foundation has potential to serve as a repairable fuse to isolate columns from large seismic demands.

3.4 CHAPTER SUMMARY

A series of centrifuge tests modeled the seismic behavior of a bridge deck mass supported by a flexible column supported on shallow foundations of various sizes. The behavior of rocking foundations was investigated using slow cyclic loading tests as well as loading due to dynamic base shaking. The moment-rotation behavior was similar for slow cyclic and dynamic loading, but the settlements were noticeably larger during dynamic shaking. The performance of a system with smaller footing (B = 3 Dc) is in some aspects preferable to the performance of systems supported on larger footings (B = 4 or 5 times Dc).

As the footing size reduces, moment and curvature ductility demands on the column and acceleration demands on the deck are reduced, but displacement demands on the deck are increased. Smaller footings do suffer greater permanent rotations and settlements than larger footings. The magnitude of settlement, however, appears to be acceptable even for the smallest footings, with permanent settlement being on the order of 30 mm (prototype scale) during large seismic events.

Contrary to what many engineers believe, the moment capacity of rocking shallow foundations is relatively straightforward to calculate. The moment rotation behavior is very ductile with no apparent loss of capacity under large-amplitude cyclic loading. Because yielding associated with rocking of shallow foundation is ductile, repairable, and includes self-centering due to closure of the gap associated with rocking, foundation rocking may be a preferred mechanism of yielding; engineers should consider the option of allowing shallow foundations to rock as a method of protecting the columns. The above conclusions are most applicable to shallow foundations on medium-dense sandy soils. Additional testing may be required prior to application to other soil types.

4 Documentation for “Soilfootingsection2d”: General Attributes of Contact Interface Model

4.1 DESCRIPTION OF CONTACT INTERFACE MODEL

This section presents a new “contact interface model” that has been developed to provide nonlinear constitutive relations between cyclic loads and displacements of the footing-soil system during combined cyclic loading (vertical, shear, and moment). The notation used for forces and displacements is indicated in Figure 4.2. The rigid footing and the soil beneath the footing in the zone of influence, considered as a macro-element, were modeled by keeping track of the geometry of the soil surface beneath the footing, the kinematics of the footing-soil system including moving contact areas and gaps. The contact interface model, with only seven user-defined model parameters, is intended to capture the essential features (load capacities, stiffness degradation, energy dissipation, and permanent deformations) of the cyclic load-deformation behavior of shallow foundations.

From the numerical modeling point of view, the contact interface model is placed at the footing-soil interface, replacing the rigid foundation and surrounding soil in the zone of influence as indicated in Figure 4.1. When incremental displacements are given to the macro-element model as input, it returns the corresponding incremental loads and vise versa. (Gajan 2006; Gajan and Kutter 2007).

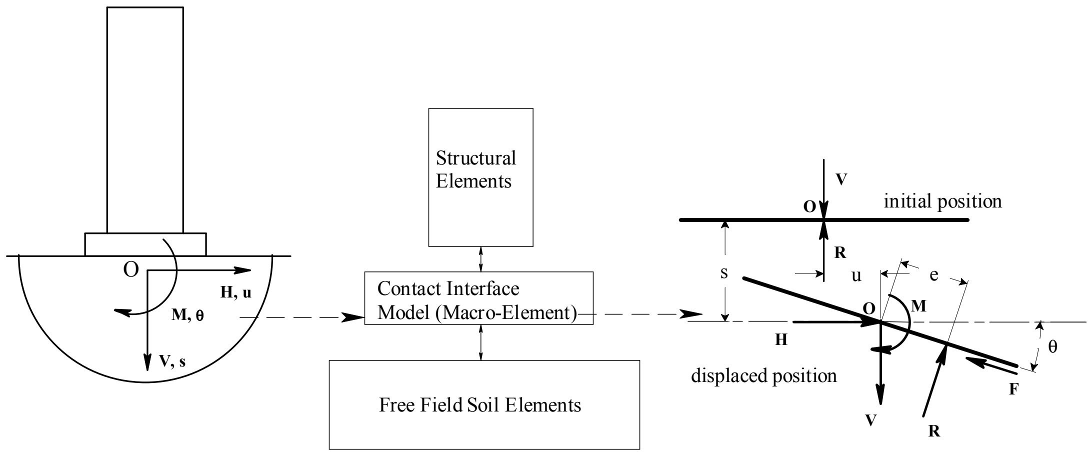

Fig. 4.1 The concept of macro-element contact interface model and the forces and displacements at footing-soil interface during combined loading (Gajan and Kutter 2007).

Other researchers have used macro-element concepts to model the load-displacement behavior of structural elements and shallow foundations (Nova and Montrasio 1991; Cremer et al. 2001; Houlsby and Cassidy 2002). Most of the previous attempts with macro-element models for shallow foundations describe the constitutive relations based on yield surfaces, potential surfaces, and tracking the load path history in generalized load space. The macro-element contact interface model presented in this paper differs in the sense that the constitutive relations are obtained by tracking the geometry of gaps and contacts of the soil-footing interface.

4.1.1 Critical Length in Contact Geometry Concepts

A conceptual key to the model is a parameter called the critical contact area ratio A/Ac, where A is the area of the footing and Ac is the area of the footing required to have contact with soil to support the vertical and shear loads. A/Ac can be considered to be an alternative definition of the factor of safety with respect to bearing capacity. Knowing the area required to support the axial and shear loads (Ac) is the key to tracking the geometry of the contact between the footing and the deformed soil surface. For a 2-D shear wall structure, loading in the plane of the wall, the area ratio, A/Ac is equal to the ratio of L/L_C, which is illustrated in Figure 4.2. At large rotations, the contact length of the footing approaches its minimum value, L_C, and assuming that the pressure distribution is symmetrical on this critical area, the resultant soil reaction is at a maximum eccentricity, $e_{max} = (L - L_C)/2$. Hence the moment capacity may be calculated as $M_{ult} = V(L - L_C)/2$, where V is the vertical load on the interface.

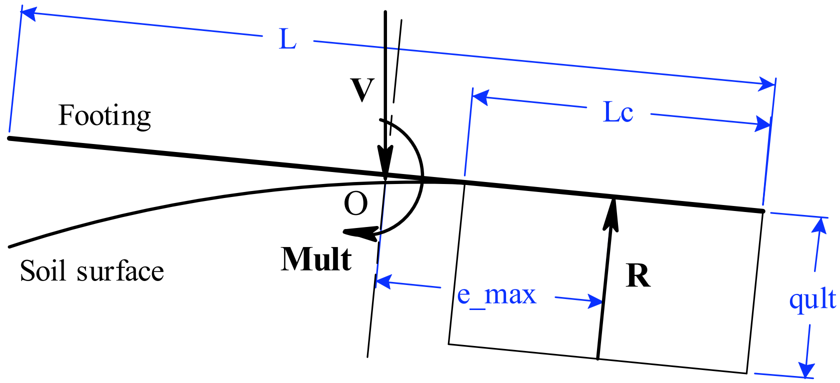

Fig. 4.2 Critical contact length and ultimate moment (Gajan 2006).

4.1.2 Curved Soil Surfaces and Rebound

Figure 4.2 illustrates the contact interface model showing the contact of the rigid footing with the rounded soil surface beneath the footing and the forces acting at the interface. As shown in Figure 4.3, soil_min and soil_max represent two different rounded soil surfaces beneath the footing. Soil_max represents the soil surface that contains the maximum settlement experienced by the footing at any point below the footing, whereas soil_min represents the surface that exists after the footing leaves the contact with the soil surface as the structure rocks. The difference between soil_max and soil_min is conceptually attributed to elastic rebound and bulging of soil into the gap associated with plastic compression in neighboring loaded areas.

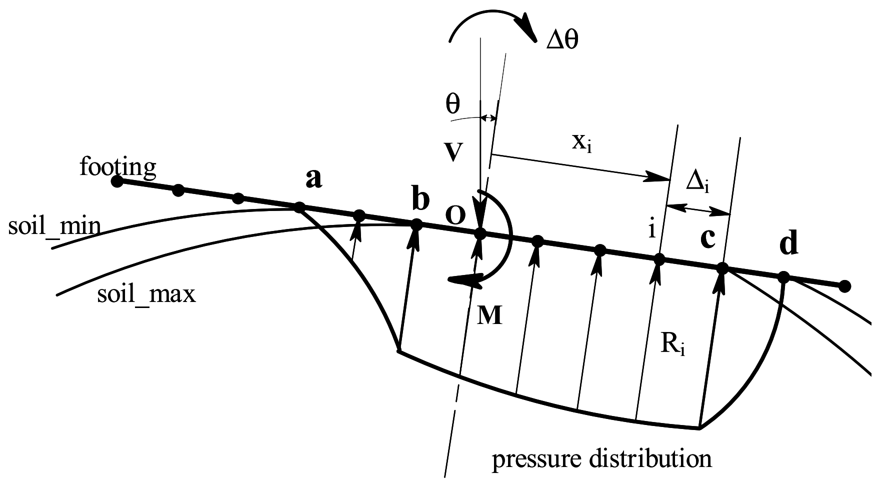

Fig. 4.3 Contact interface model for cyclic moment loading (Gajan and Kutter 2007).

4.1.3 Coupling between Shear, Moment and Vertical Loads, and Displacements

The coupling between vertical and moment loads and associated deformations is a natural outcome of tracking the geometry of the contact between a rigid footing and deformed soil. The coupling between shear and moment is accounted for using the interaction diagram in Figure 4.4.

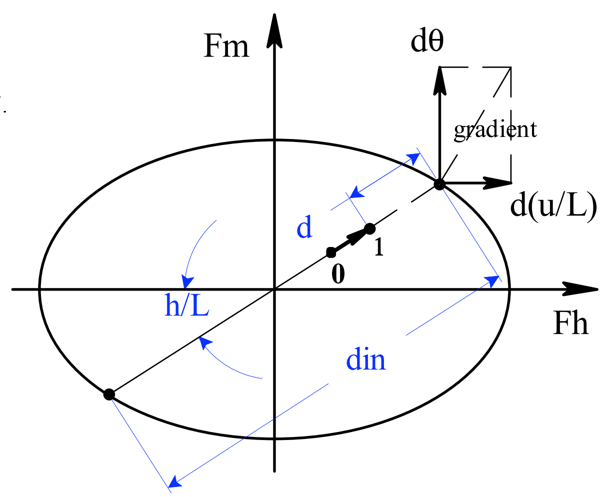

Fig 4.4 Cross section of the bounding surface in normalized M-H plane and the geometrical parameters that are used in the interface model (Gajan and Kutter 2007).

The magnitude of the sliding is a function of the shear on the footing and the proximity to the bounding surface, which is quantified by the ratio of (d/din). The shear stiffness is a function of (d/din), which determines the shape of the nonlinear transition from the initial stiffness to capacity for the shear-sliding relationship of the footing. The bounding surface in Figure 4.4 not only describes the interaction between moment and shear capacities, but also relates the incremental rotations to the incremental sliding by assuming associative flow. The procedures for calculating load capacities and displacements are detailed in Gajan and Kutter (2007) and Gajan (2006).

4.2 IDENTIFICATION OF PARAMETERS

The description of model parameters will be broken up into user-defined input parameters and non-user-defined parameters.

4.2.1 User-Defined Input Parameters and Parameter Selection Protocols

Input parameters for "soilfootingsection2D" are ultimate vertical load, length of footing, initial vertical stiffness, initial horizontal stiffness, elastic rotation limit, rebound ratio, and internal node spacing. The effect of most physical parameters (V_{ULT}, L, Kv, and Kh) on the load-deformation behavior of the footing is explored in detail in Gajan (2006) and only the effects of parameters controlling numerical stability have been shown in conjunction with the parameter selection protocols below. The following list describes the input parameters and recommended protocols for how to calculate them.

1. **Ultimate vertical load (V_{ULT}):** The maximum vertical load that can be applied to the footing with the full footing in contact, corresponding to a bearing capacity failure. Calculate V_{ULT} for the footing under pure vertical loading using the general bearing capacity equation for the footing in full contact with soil (FEMA 274) in units of force.
2. **Length of footing (L):** The linear dimension of the footing in the plane of rocking.
3. **Initial vertical stiffness (Kv):** The initial vertical stiffness of the footing in full contact with soil for pure vertical loading. This may be taken as the elastic vertical stiffness of the entire footing in units of force/displacement from FEMA 356, Chapter 4, elastic solutions for Rigid Footing Spring Constraints.

4. **Initial horizontal stiffness (Kh):** The elastic shear stiffness of the footing in full contact with the soil for pure shear loading. This may be taken as the elastic horizontal stiffness of the entire footing in units of force/displacement from FEMA 356 Chapter 4 elastic solutions for Rigid Footing Spring Constraints.
5. **Elastic rotation limit ($\theta_{elastic}$):** The maximum amplitude of rotation for which no settlements occur. This elastic range was introduced by Gajan and Kutter (2009) subsequent to Gajan et al. (2005), and Gajan (2006). This may be taken as 0.001 rad, as this has shown to match centrifuge experiments reasonably well. If $\theta_{elastic}$ is too small the model will predict an unreasonable amount of settlement during the small amplitude shaking at the beginning and end of an earthquake. Figure 4.5 illustrates the observed physical behavior modeled by the introduction of the parameter $\theta_{elastic}$. During small rotations the model is forced to not uplift as observed in experiments.

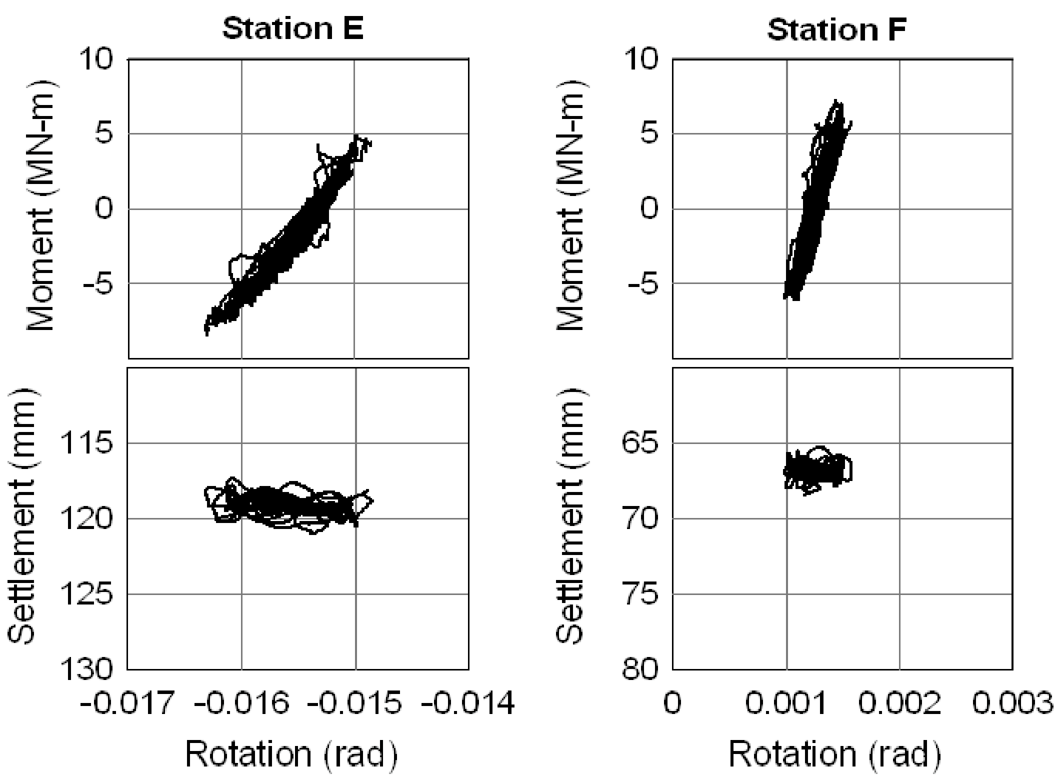

Fig. 4.5 Elastic range for two identical structures on different sized footings.

6. **Rebound ratio (Rv):** An empirical factor to account for the elastic rebound and the bulging of soil into the gap associated with plastic compression in neighboring loaded areas described in Section 4.1.2. The model assumes that the amount of rebound is

proportional to the total settlement computed by the element. For example, if Rv is 0.1, any gap between the uplifting footing and soil surface smaller than 10% of the previous settlement would be filled by rebounding soil and the distance between soil_max and soil_min is at any point is 10% of the settlement of that point.

A default value of 0.1 has been used for many simulations, as it reasonably fits the current data from centrifuge model tests for rectangular and square footings on sand and clay. An increase in Rv will slightly reduce calculated settlements and increase rotational stiffness.

In cases where convergence is a problem, especially with footings with large FS_V and an extreme amount of load cycles, increasing Rv can increase the length of the transition zone shown in Figure 4.3 of the pressure distribution under the footing, making convergence easier. The use of Rv as a parameter to control numerical stability is shown in Figure 4.6. It should be noted that increasing Rv does not always make the model more stable. Increasing Rv will stiffen the load-deformation response, which can make the model less stable in some situations.

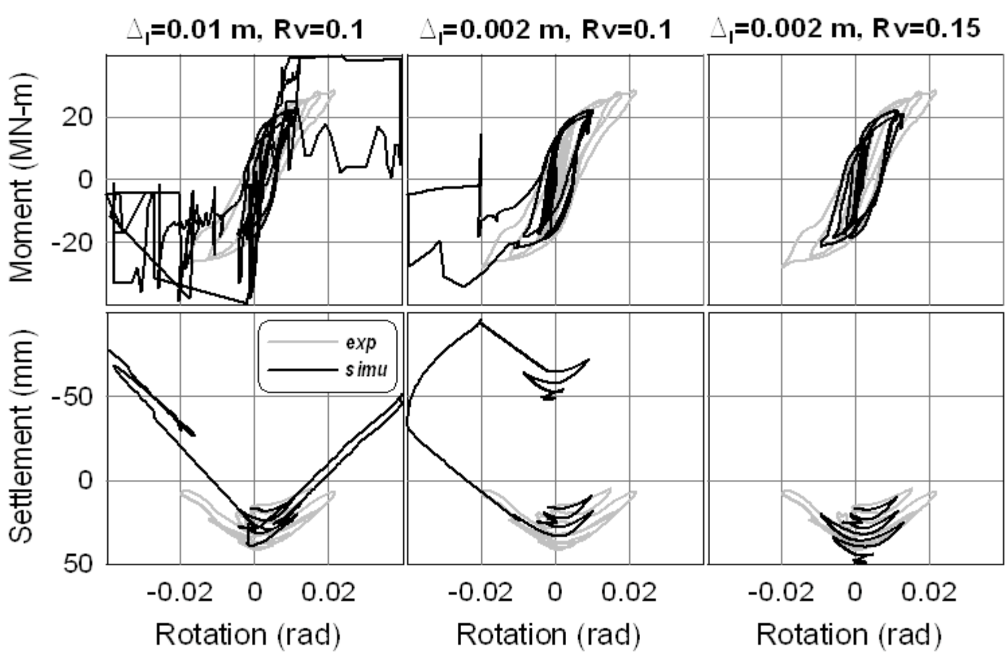

Fig. 4.6 Effect of D_l and Rv on moment-rotation and settlement-rotation of footing.

7. **Footing Node Spacing (D_l):** The distance between the footing nodes internally created in the model (Fig. 4.3). This user-defined parameter controls numerical stability and accuracy.

   Depending on the model properties, different numbers can be appropriate. As the critical contact length (L_C) decreases (or as FS_V increases) D_l must be small enough to define the pressure distribution along the soil-footing contact length depicted in Figure 4.3. For a large range of L and FS_V, D_l of 0.01 m provides stable and accurate results. The number of internally created footing nodes necessary for numerical stability and accuracy will range from a few hundred nodes for FS_V below 10 to a few thousand for FS_V of 50. For example, a footing of length 5 meters with a D_l of 0.01 m will have 501 internally created footing nodes. Computation time is extremely sensitive to this input parameter.

   If D_l is too large, many times the footing will start to accumulate uplift instead of a net settlement. This occurs because the pressure distribution along the contact length is not defined by enough nodes; specifically, nodes b and c in Figure 4.4 are in the same location. If the footing is seen to have a net uplift for any cycle then D_l is too large as is the case in Figure 4.7.

4.2.2 Summary of Parameters Assumed To Be Constants

This list describes parameters that are hard-wired into the code [more on these can be found in Gajan et al. 2005; Gajan 2006; Gajan and Kutter 2007 and in the source code (/SRC/material/section/yieldsurface/ soilfootingsection2D*)]:

1. n_load = 0.5, n_unload = 2: describe the limiting shape of the parabolic pressure distribution at the edges of the contact length between points a and b and c and d in Figure 4.3. When loading direction is reversed, there is a smooth transition in the shape (from n = 0.5 to n = 2) given by the following equations:

$$n\_load = 1.5 \cdot \left(\frac{\theta - \theta_{elastic}}{2 \cdot \theta_{elastic}} \right) + 0.5 \tag{4.1}$$

$$n\_unload = 1.5 \cdot \left(\frac{\theta_{elastic} - \theta}{2 \cdot \theta_{elastic}} \right) + 0.5 \tag{4.2}$$

2. a = 0.32, b = 0.37, c = 0.25, d= 55, e = 0.8 and f = 0.8: define the bounding surface in normalized moment-shear-vertical load space (Cremer et al. 2001). The bounding surface is defined by the following three equations:

$$\frac{F_H{}^2}{A^2}+\frac{F_M{}^2}{B^2}=1 \tag{4.3}$$

$$A=a\cdot F_V{}^c\cdot(1-F_V)^d \tag{4.4}$$

$$B=b\cdot F_V{}^e\cdot(1-F_V)^f \tag{4.5}$$

where F_H, F_M, and F_V are the normalized shear, moment, and vertical capacities of the foundation-soil interface. ($F_V = V/V_{ULT}$, $F_H = H/V_{ULT}$ and $F_M = M/(V_{ULT}\,L)$, and V_{ULT} is failure load for pure vertical loading). This bounding surface was verified with centrifuge tests.

3. c = 1, n = 2: coefficient and exponent describing the sharpness of the transition between elastic and plastic behavior for shear-sliding. These parameters were selected by comparing to a variety of data and were not found to be critical parameters.

5 Validation against Centrifuge Tests on Bridge Columns on Square Footings

5.1 CENTRIFUGE TESTS ON BRIDGE COLUMNS

The scope and procedures relevant to the centrifuge structures modeled numerically will be described herein to provide a background for the comparisons to the numerical simulations although more details about the test setup, the testing, and the data processing procedures can be found in Chapter 2 and in the Centrifuge Data Report for the JAU01 Test Series (Ugalde et al. 2008).

Testing was performed on many model structures which were placed into one soil container. The structures were spaced so that they were an adequate distance from each other and the walls of the container. Stations C through G were excited by ground motions applied to the base of the soil container.

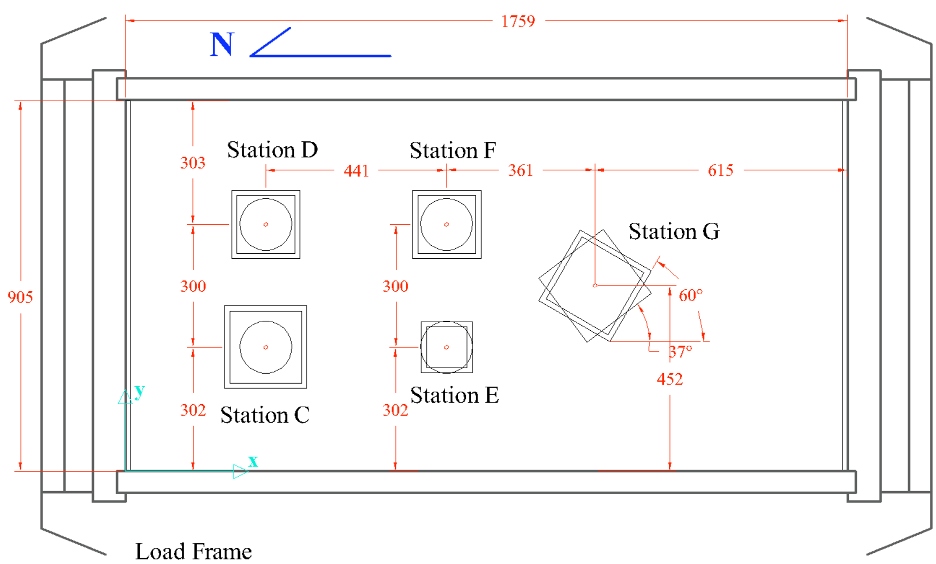

Fig. 5.1 Plan view of dynamic shaking stations where double line borders indicate footings and single lines indicate deck masses.

The two structures used in the verification of the contact interface model are at Stations E and F. These two structures were shaken side by side and are identical except for the different footing sizes. The properties are shown in Table 5.1. The masses and moments of inertia specified for the footing and bridge deck come from summing the mass of everything above the midpoint of the column as the deck mass and everything below the midpoint of the column as the footing mass.

Table 5.1 Structure properties used to calculate experimental load-deformation behavior.

Station	FS_V	Deck Mass (Mg)	Footing Mass (Mg)	Footing Width (Square) (m)	Icg Deck ($kg*m^2$)	Icg Foot ($kg*m^2$)	Hcg deck (m)	Hcg foot (m)	Icolumn (m^4)	Ecolumn (Pa)
E	17	926	173	5.4	3.34E+06	8.67E+05	13.47	1.215	1.07E-01	6.90E+10
F	31	926	246	7.1	3.34E+06	1.93E+06	13.47	1.238	1.07E-01	6.90E+10

Structures at Stations E and F were subject to dynamic loading using the shaking table mounted on the centrifuge to shake the entire model container. The ground motions imposed on the model container were scaled and filtered motions from recordings in the Tabas 1978 earthquake and a Los Gatos recording of the 1989 Loma Prieta earthquake. These motions come from the near-field records posted at the SAC Steel Project (2006) website. Twelve scaled motions were applied to each structure. The testing sequence for dynamic stations started with low-amplitude step waves, followed by scaled-down earthquake ground motions, then large-amplitude earthquake ground motions, and finally step waves similar to those applied before strong shaking. The peak ground accelerations ranged between 0.1 g and 0.8 g.

The motions used in the comparison of the measured physical response and the simulated response were the fifth, sixth, and eighth events of the fifth spin of the JAU01 test series. Shaking events five, six, and eight were chosen because the low-intensity events 1, 2, 3, 4, and 7 resulted in very little settlement or nonlinear load-deformation of the footing. The motion recorded at the footing level in free field during the experiment was used as input at the base of the contact interface element.

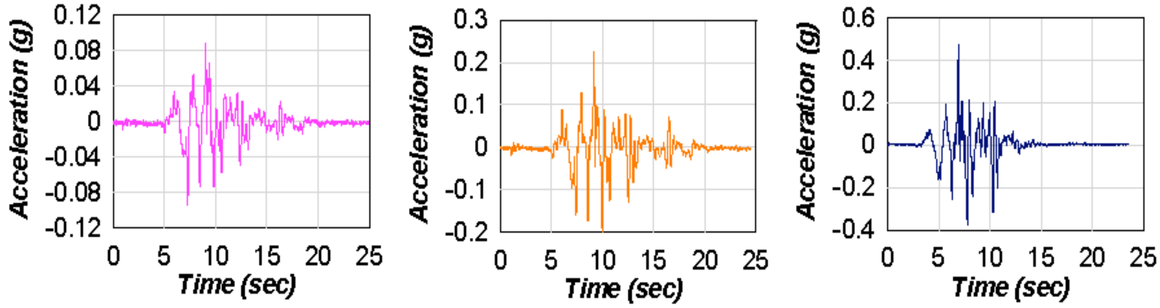

Fig. 5.2 Acceleration time history of free-field soil at footing level for motions during event (a)JAU01_05_05, (b) JAU01_05_06, and (c) JAU01_05_08.

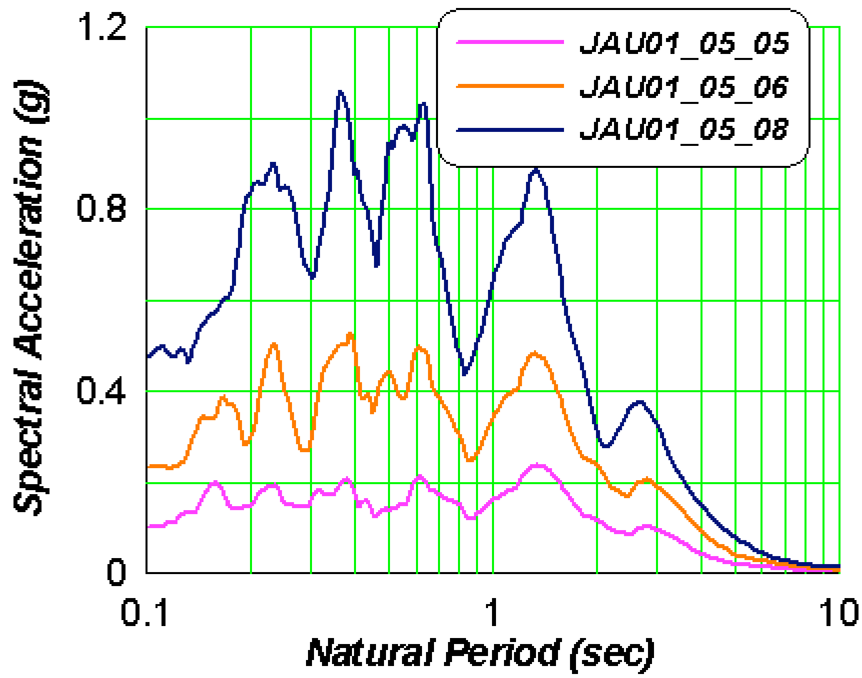

Fig. 5.3 Acceleration response spectra (for 5% damping ratio).

5.2 EXPERIMENTAL AND NUMERICAL MODELING RESULTS

A schematic of the structural model is shown in Figure 5.4. Five structural nodes are used in the simplified numerical model of the simplified physical model used in the centrifuge tests. These five nodes are located at the base of the footing, the center of gravity of the footing mass, the height to the fixity point at the base of the column, the height to the fixity point at the top of the column, and the center of gravity of the deck mass. All structural elements are elastic beam-columns. The element representing the structure column was given the properties of the aluminum tube used in the centrifuge test. The elements extending to the deck mass, the footing mass, and the column fixity points are all approximately rigid by using elastic beam-columns with 20 times the area moment of inertia, I, of the column.

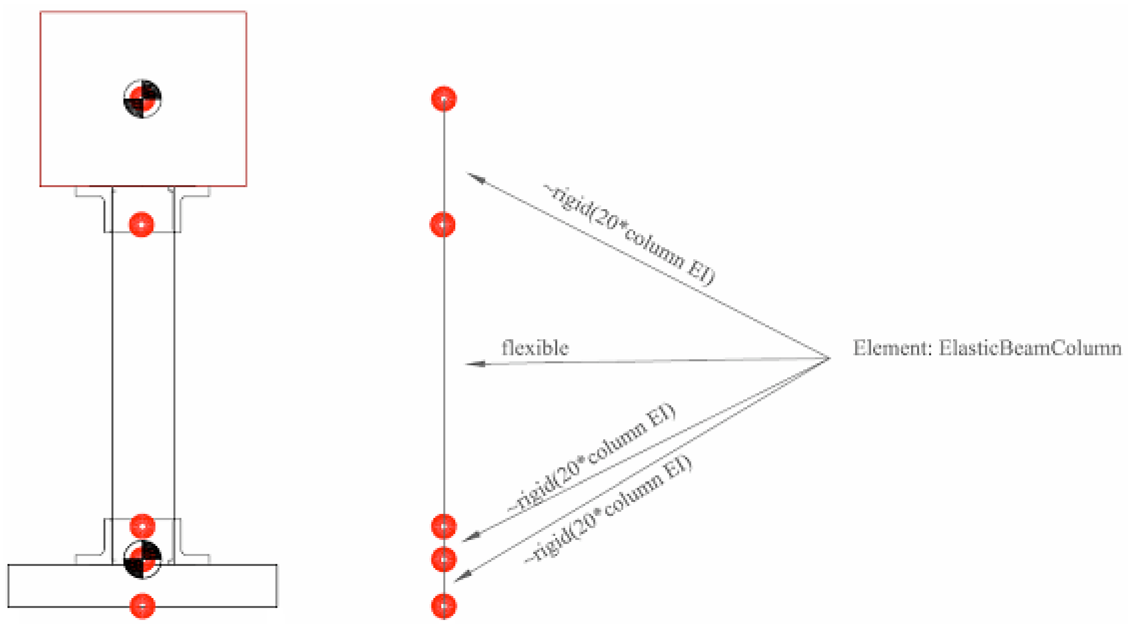

Fig. 5.4 Simplified structural numerical model of experiment.

5.2.1 Contact Interface Element Results

The contact interface element results describe the footing behavior when the structure in Figure 5.4 is supported by the contact interface model implemented in the section soilfootingsection2D and is used in the zero length section below the footing. "The following figures (Figs. 5.5–5.10) show the load-deformation response as well as significant structural time histories of the two footings to three consecutive earthquake motions. The measured experimental results are compared to the behavior simulated using the contact interface element in OpenSees (OpenSees Development Team 2007).

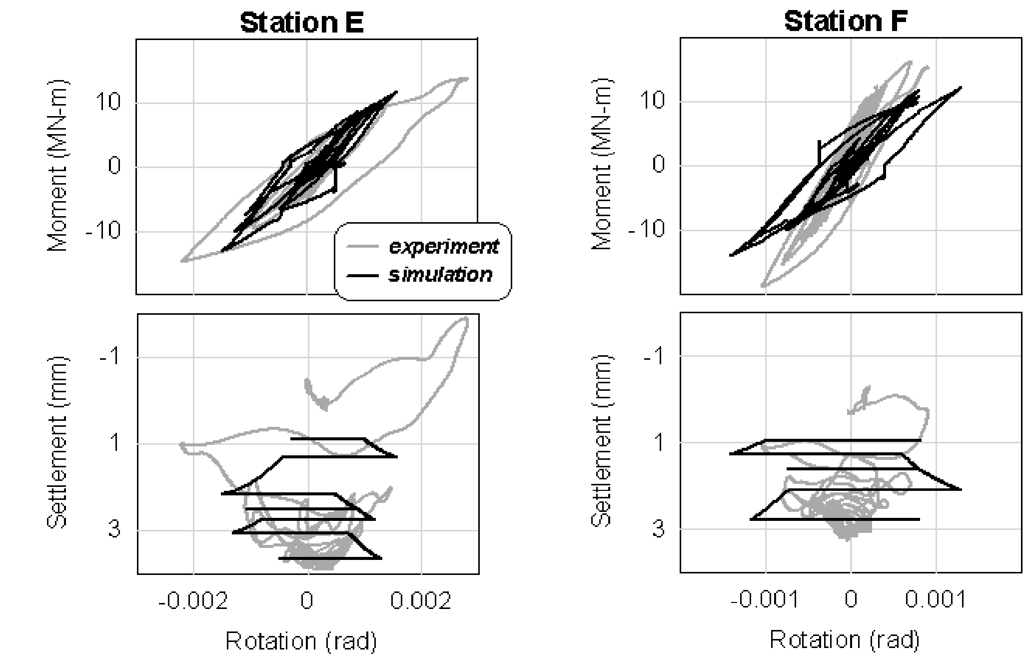

Fig. 5.5 Load-deformation behavior of footing for (a) Station E and (b) Station F during JAU01_05_05.

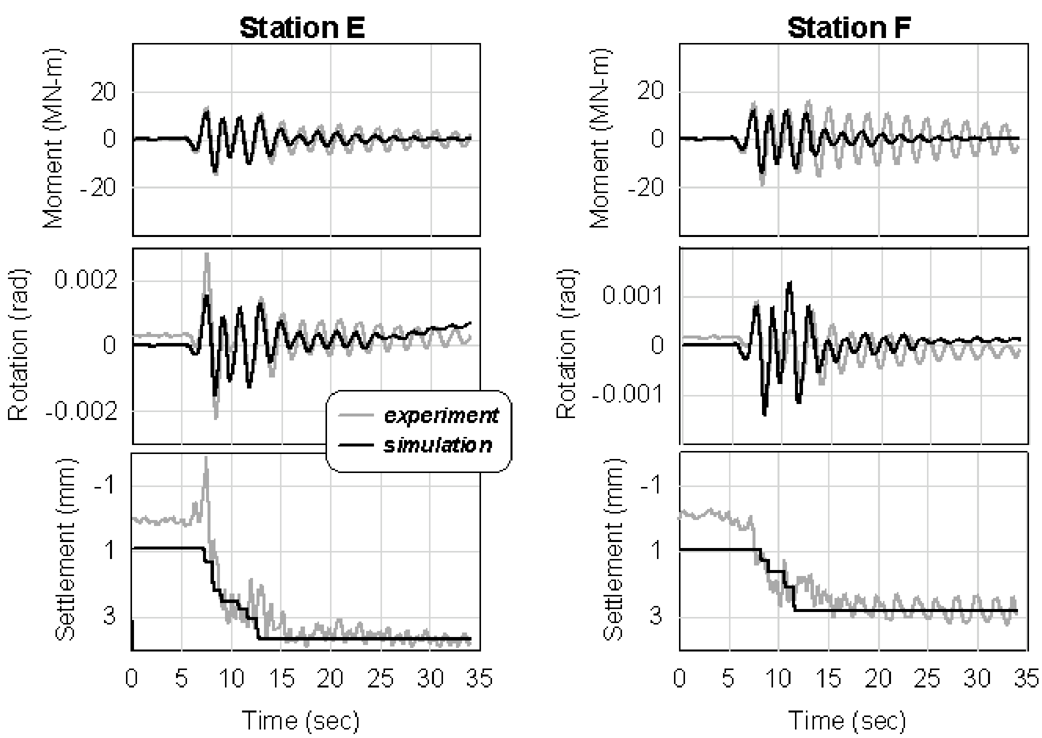

Fig. 5.6 Footing moment, rotation, and settlement time histories for (a) Station E and (b) Station F during JAU01_05_05.

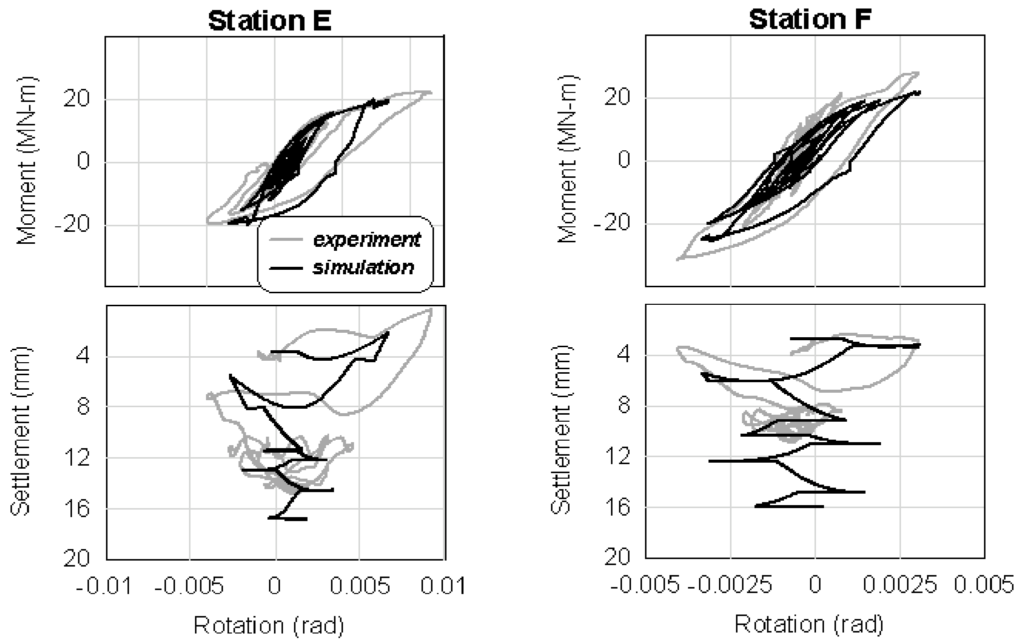

Fig. 5.7 Load-deformation behavior of footing for (a) Station E and (b) Station F during JAU01_05_06.

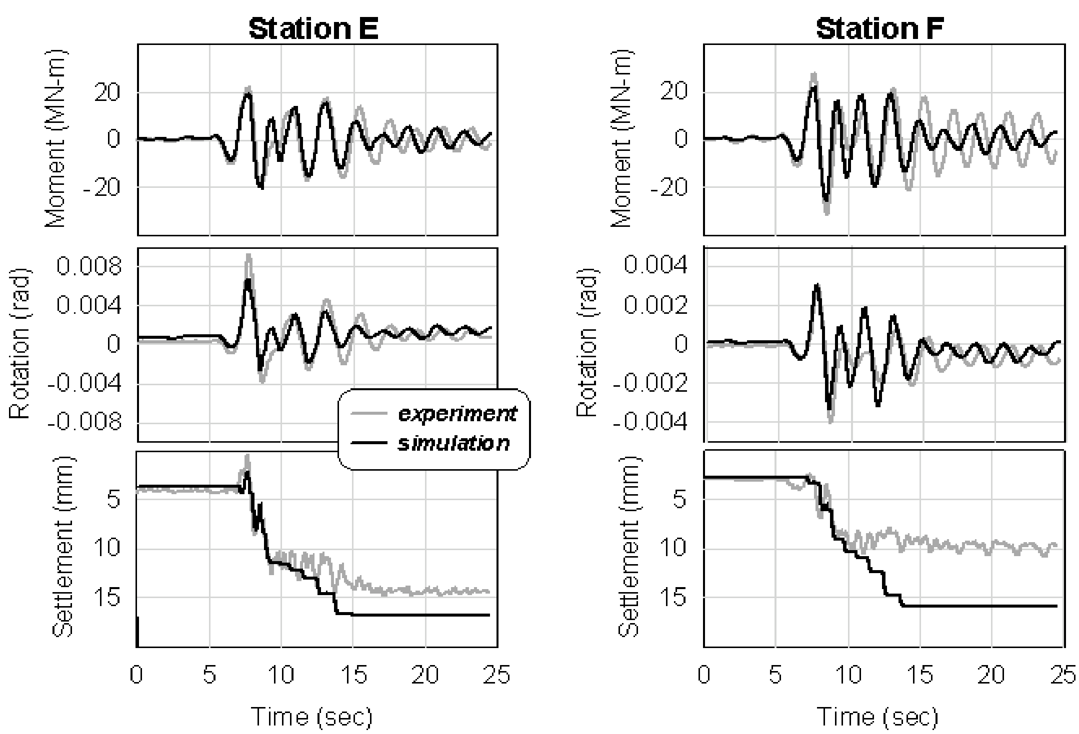

Fig. 5.8 Footing moment, rotation, and settlement time histories for (a) Station E and (b) Station F during JAU01_05_06.

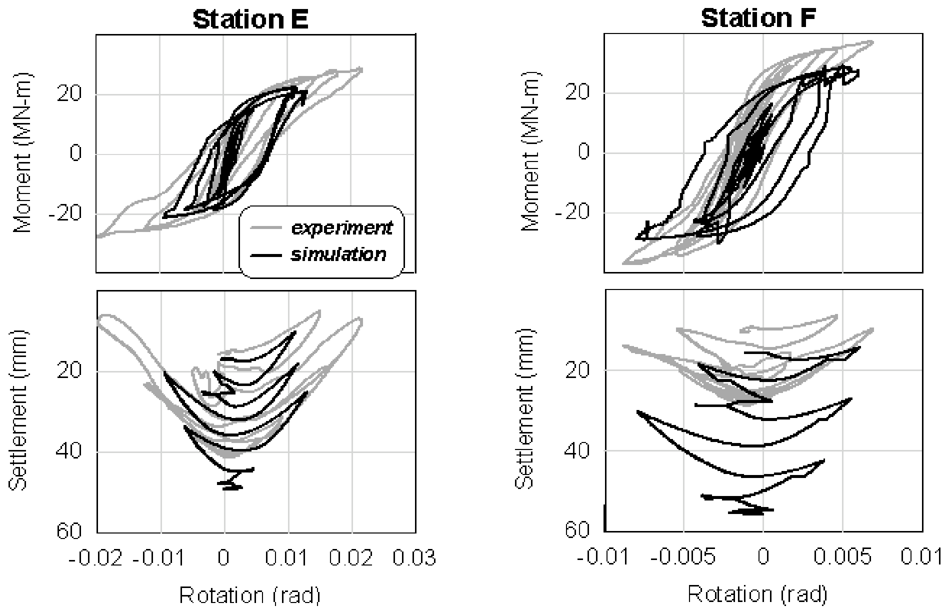

Fig. 5.9 Load-deformation behavior of footing for (a) Station E and (b) Station F during JAU01_05_08.

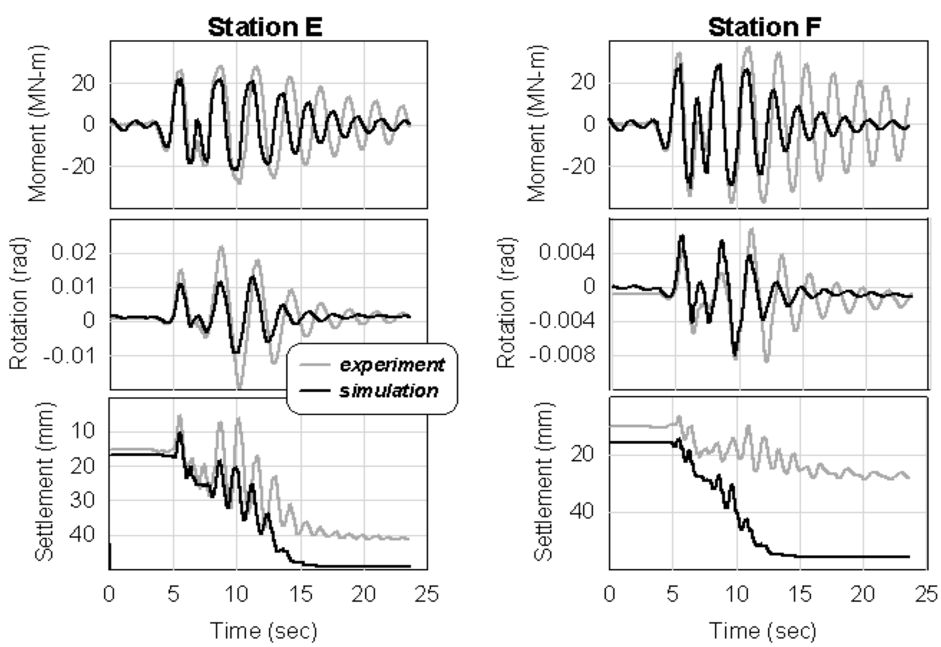

Fig. 5.10 Footing moment, rotation, and settlement time histories for (a) Station E and (b) Station F during JAU01_05_08.

5.3 SUMMARY

5.3.1 Load Capacity

The moment capacity of the footing is underpredicted by the contact interface model for both Station F and Station E in for all events. This may be partly due to the 6% Rayleigh damping introduced to satisfy convergence issues.

5.3.2 Energy Dissipation

The energy dissipated by moment-rotation hysteresis is captured reasonably well by the contact interface model, although the Rayleigh damping introduced into the simulation inhibits the footing response after strong shaking is finished.

5.3.3 Footing Displacements

During small shaking the magnitude of permanent settlement is predicted reasonably well. However, the simulated response of the larger footing (Station F) to the more intense earthquakes (JAU01_05_06 and JAU01_05_08) shows permanent settlements are overpredicted. The contact interface model does much better at predicting the permanent settlement of Station E, the smaller footing, although the magnitude of the cyclic uplift is underpredicted and permanent rotations at zero moment is overpredicted.

6 Summary and Conclusions

6.1 CONCLUSIONS

It is clear that the soil beneath a shallow foundation as a component of the soil-foundation-structure system should be considered a possible location where inelastic behavior can be designed to occur. The design of a rocking shallow foundation could conform to the analysis requirements described in Caltrans Memo to Designers (MTD) 20-1 under Seismic Capacity of Structural Components. The requirement that finite element analysis be used to calculate the strength and the deformation capacities of ductile components is possible using the models available in the free open-source code OpenSees. The requirement of the ductile region to be designed and detailed to perform with minimal degradation in strength to sustained cyclic loading has been shown in multiple experiments on sand and clay for rectangular and square footings with vertical factors of safety on bearing capacity ranging from below 2 to above 30 (Gajan and Kutter 2007; Ugalde et al. 2007).

In many ways the load-deformation behavior of a rocking foundation is arguably a better energy-dissipation mechanism compared to the conventional reinforced concrete column. The moment capacity of the reinforced concrete column degrades, while the moment capacity of the shallow foundation does not diminish with rotation amplitude or number of cycles. A reinforced concrete column has a very stiff unloading response resulting in much more permanent deformation than seen in the rocking shallow foundation. Although the behavior of a reinforced concrete column and shallow foundation vary depending on the properties of the structure and soil, in general the trends of cyclic fatigue and large permanent deformations are not present in the shallow foundations tested. Figures 6.1 and 6.2 illustrate the differences in hysteresis loops of a reinforced concrete column and a shallow foundation.

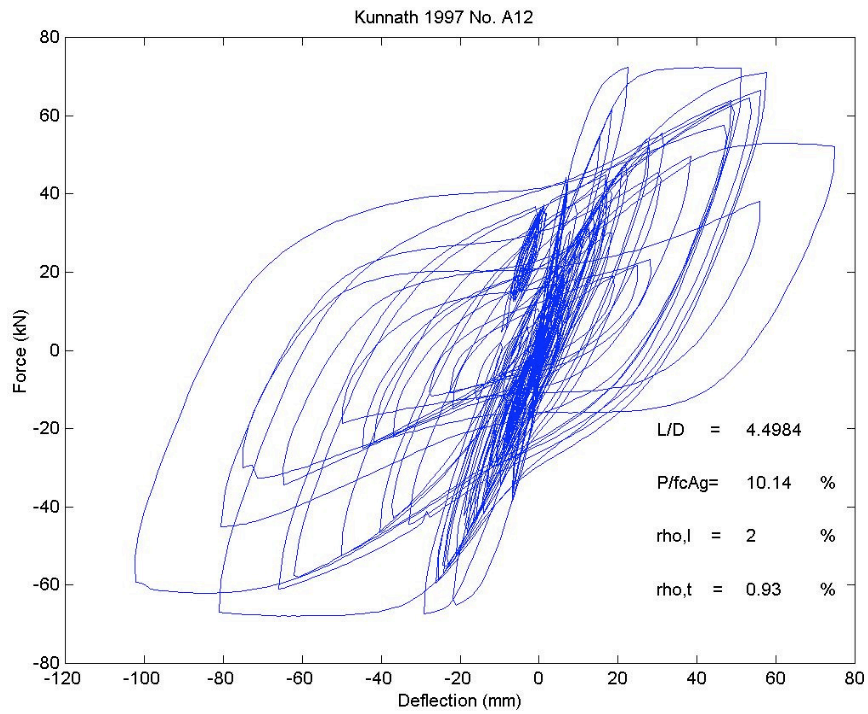

Fig. 6.1 Lateral load-deformation response of reinforced concrete column (Kunnath et al. 1997).

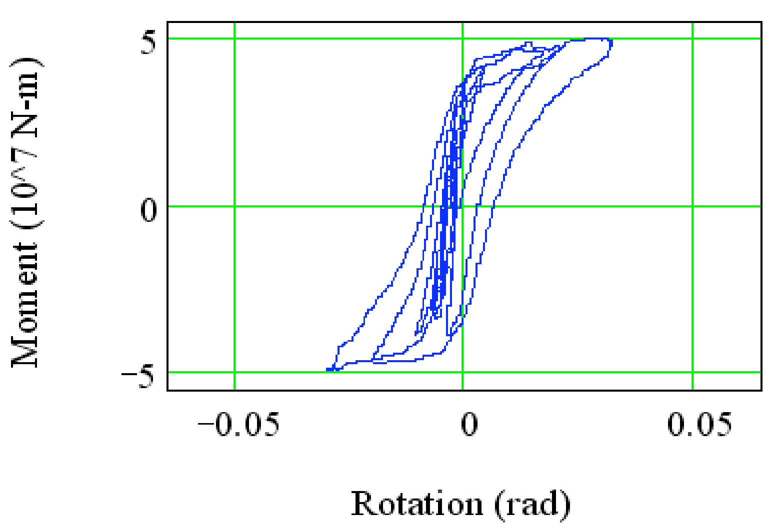

Fig. 6.2 Load-deformation response of a rocking shallow foundation during dynamic ground shaking. (Ugalde et al. 2007).

Caltrans MTD 20-1 should have a larger scope on Soil-Foundation-Structural Components. Also, the recommendation is that the Caltrans Technical Report *Bridge Retrofit Construction Techniques* be updated to include the possibility that foundation uplift be allowed as long as the global ductility capacity is greater than the anticipated demand.

Furthermore, in fulfilling existing requirements for ductile components, a shallow foundation has the following benefits:

A footing designed to uplift is inexpensive.

There is no failed component to inspect after an earthquake, as soil is made up of broken particles.

Unlike concrete, soil derives strength from friction and not a cohesion that disappears upon cracking, which means that the moment capacity is nondegrading and easily predicted in unsaturated medium-dense sandy soils.

Uplift of a foundation stores gravitational potential energy. Closure of the gap upon unloading restores the footing toward its initial position (unlike a conventional RC column), producing a self-centering effect.

Local bearing pressures increase during rocking and uplift, causing plastic deformation of soil around the footing, which is a source of hysteretic damping.

Experiments with structures on footings that were allowed to uplift were observed to perform reasonably well with no stability problems or excessive P-delta effects after multiple shaking events.

REFERENCES

Alameddine F, Imbsen R (2002). "Rocking of bridge piers under earthquake loading," Proceedings of the Third National Seismic Conference & Workshop on Bridges and Highways.

Butterfield R., Houlsby GT, Gottardi, G (1997). "Standardized sign conventions and notation for generally loaded foundations," Geotechnique, 47, No. 5, 1051-1054.

Caltrans (2006). *Seismic design criteria*. Version 1.4 http://www.dot.ca.gov/hq/esc/techpubs/manual/othermanual/other-engin-manual/seismic-design-criteria/sdc.html

Caltrans (2004). *Bridge Design Specifications*. September. http://www.dot.ca.gov/hq/esc/techpubs/manual/bridgemanuals/bridge-design-specifications/bds.html

Caltrans (2003). *Memo To Designers 4-1*. November. http://www.dot.ca.gov/hq/esc/techpubs/manual/bridgemanuals/bridge-memo-to-designer/page/Section%204/4-1m.pdf

Caltrans (1999). *Memo To Designers 20-1*. January. http://www.dot.ca.gov/hq/esc/techpubs/manual/bridgemanuals/bridge-memo-to-designer/page/Section%2020/20-1m.pdf

Chopra AK (2001). *Dynamics of structures: Theory and applications to earthquake engineering*, Prentice Hall, Upper Saddle River, New Jersey, pp. 104.

Cremer C, Pecker A, Davenne L (2001). "Cyclic macro-element for soil-structure interaction: material and geometrical non-linearities," International Journal for Numerical and Analytical Methods in Geomechanics, 25, pp. 1257-1284.

Faccioli E, Paolucci R, and Vivero G (2001). "Investigation of seismic soil-footing interaction by large-scale cyclic tests and analytical models," In Proc. Fourth International Conference on Recent Advances in Geotechnical Earthquake Engineering and Soil Dynamics, San Diego, March 26-31.

Gajan S, Phalen JD, Kutter BL, Hutchinson TC, and Martin G (2005). "Centrifuge modeling of the load deformation behavior of rocking shallow foundations," Journal of Soil Dynamics and Earthquake Engineering, 25, 773–783.

Gajan S (2006). "Physical and numerical modeling of nonlinear cyclic load-deformation behavior of shallow foundations supporting rocking shear walls," Ph.D. Thesis. University of California at Davis, College of Engineering.

Gajan, S. and Kutter, B.L. (2009). "Contact interface model for shallow foundations subjected to combined cyclic loading", J. Geotech and Geoenv. Engr., ASCE 135(3), 407-419.Georgiadis M, Butterfield R (1988). "Displacements of footings on sand under eccentric and inclined loads," Canadian Geotechnical Journal, 25, 199-211.

Hipley P (1997). "Bridge retrofit construction techniques," Office of Earthquake Engineering-Seismic Technology Section. Presented at the Second National Seismic Conference on Bridges and Highways.

Houlsby GT, Cassidy MJ (2002). "A plasticity model of the behaviour of footings on sand under combined loading," Geotechnique, 52, No. 2, pp. 117-129.

Housner GW (1963). "The Behavior of Inverted Pendulum Structures During Earthquakes," Bulletin of the Seismological Society of American, Vol. 53, No.2, pp. 403-417.

Hu, G (2006). “Rocking of shallow foundations,” M.S. Thesis. University of California at Davis, College of Engineering.

Kutter BL (1995). "Recent Advances in Centrifuge Modeling of Seismic Shaking," State-of-the-Art Paper, Proceedings, Third International Conference on Recent Advances in Geotechnical Earthquake Engineering and Soil Dynamics, St. Louis, MO, Vol.2, pp. 927-942, April.

Kunnath SK., El-Bahy A, Taylor A, Stone W (1997). “Cumulative seismic damage of reinforced concrete bridge piers,” Technical Report NCEER-97-0006, National Center for Earthquake Engineering Research, September.

Mergos P, Kawashima K (2005). "Rocking isolation of a typical bridge pier on spread foundation," Journal of Earthquake Engineering, Vol. 9. Special Issue 2, pp 395-414.

OpenSees Development Team (Open Source Project, 2007). “Open system for earthquake engineering simulation (OpenSees),” http://opensees.berkeley.edu/.

Priestley NMJ, Seible F and Calvi GM (1996). *Seismic design and retrofit of bridges*, John Wiley & Sons.

SAC Steel Project (2006) Impulsive Near-Field Earthquake Ground Motions http://nisee.berkeley.edu/data /strong_motion/sacsteel/motions/nearfault.html

Sakellaraki D, Watanabe G, Kawashima K (2005). “Experimental rocking response of direct foundations of bridges.” Second International Conference on Urban Earthquake Engineering, pp. 497-504.

Schofield AN (1980). “Cambridge geotechnical centrifuge operations”, Rankine Lecture, Geotechnique, v 30, n 3 , p 227-268.

Taylor PW, Bartlett PE, and Weissing PR (1981). “Foundation rocking under earthquake loading,” 10th International Conference on Soil Mechanics and Foundation Engineering, Vol. 3. 313–322.

Ugalde JA, Kutter BL, Jeremić B, Gajan S. (2007). "Centrifuge modeling of rocking behavior of bridges on shallow foundations." 4th International Conference on Earthquake Geotechnical Engineering, June.

Ugalde JA, Kutter BL, Jeremić B. (2008, in press). "Soil-foundation-structure interaction: Shallow foundations.” Centrifuge Data Report for test series JAU01. Center for Geotechnical Modeling, University of California, Davis.

Wood, DM, (2004) *Geotechnical Modeling.* Spoon Press.

Zhang J, Makris N (2001). “Rocking response of free-standing blocks under cycloidal pulses.” Journal of Engineering Mechanics. May, pp 473.

PEER REPORTS

PEER reports are available individually or by yearly subscription. PEER reports can be ordered at http://peer.berkeley.edu/publications/peer_reports.html or by contacting the Pacific Earthquake Engineering Research Center, 1301 South 46th Street, Richmond, CA 94804-4698. Tel.: (510) 665-3448; Fax: (510) 665-3456; Email: peer_editor@berkeley.edu

PEER 2009/03 *The Integration of Experimental and Simulation Data in the Study of Reinforced Concrete Bridge Systems Including Soil-Foundation-Structure Interaction.* Matthew Dryden and Gregory L. Fenves. November 2009.

PEER 2009/02 *Improving Earthquake Mitigation through Innovations and Applications in Seismic Science, Engineering, Communication, and Response. Proceedings of a U.S.-Iran Seismic Workshop.* October 2009.

PEER 2009/01 *Evaluation of Ground Motion Selection and Modification Methods: Predicting Median Interstory Drift Response of Buildings.* Curt B. Haselton, Ed. June 2009.

PEER 2008/10 *Technical Manual for Strata.* Albert R. Kottke and Ellen M. Rathje. February 2009.

PEER 2008/09 *NGA Model for Average Horizontal Component of Peak Ground Motion and Response Spectra.* Brian S.-J. Chiou and Robert R. Youngs. November 2008.

PEER 2008/08 *Toward Earthquake-Resistant Design of Concentrically Braced Steel Structures.* Patxi Uriz and Stephen A. Mahin. November 2008.

PEER 2008/07 *Using OpenSees for Performance-Based Evaluation of Bridges on Liquefiable Soils.* Stephen L. Kramer, Pedro Arduino, and HyungSuk Shin. November 2008.

PEER 2008/06 *Shaking Table Tests and Numerical Investigation of Self-Centering Reinforced Concrete Bridge Columns.* Hyung IL Jeong, Junichi Sakai, and Stephen A. Mahin. September 2008.

PEER 2008/05 *Performance-Based Earthquake Engineering Design Evaluation Procedure for Bridge Foundations Undergoing Liquefaction-Induced Lateral Ground Displacement.* Christian A. Ledezma and Jonathan D. Bray. August 2008.

PEER 2008/04 *Benchmarking of Nonlinear Geotechnical Ground Response Analysis Procedures.* Jonathan P. Stewart, Annie On-Lei Kwok, Yousseff M. A. Hashash, Neven Matasovic, Robert Pyke, Zhiliang Wang, and Zhaohui Yang. August 2008.

PEER 2008/03 *Guidelines for Nonlinear Analysis of Bridge Structures in California.* Ady Aviram, Kevin R. Mackie, and Božidar Stojadinović. August 2008.

PEER 2008/02 *Treatment of Uncertainties in Seismic-Risk Analysis of Transportation Systems.* Evangelos Stergiou and Anne S. Kiremidjian. July 2008.

PEER 2008/01 *Seismic Performance Objectives for Tall Buildings.* William T. Holmes, Charles Kircher, William Petak, and Nabih Youssef. August 2008.

PEER 2007/12 *An Assessment to Benchmark the Seismic Performance of a Code-Conforming Reinforced Concrete Moment-Frame Building.* Curt Haselton, Christine A. Goulet, Judith Mitrani-Reiser, James L. Beck, Gregory G. Deierlein, Keith A. Porter, Jonathan P. Stewart, and Ertugrul Taciroglu. August 2008.

PEER 2007/11 *Bar Buckling in Reinforced Concrete Bridge Columns.* Wayne A. Brown, Dawn E. Lehman, and John F. Stanton. February 2008.

PEER 2007/10 *Computational Modeling of Progressive Collapse in Reinforced Concrete Frame Structures.* Mohamed M. Talaat and Khalid M. Mosalam. May 2008.

PEER 2007/09 *Integrated Probabilistic Performance-Based Evaluation of Benchmark Reinforced Concrete Bridges.* Kevin R. Mackie, John-Michael Wong, and Božidar Stojadinović. January 2008.

PEER 2007/08 *Assessing Seismic Collapse Safety of Modern Reinforced Concrete Moment-Frame Buildings.* Curt B. Haselton and Gregory G. Deierlein. February 2008.

PEER 2007/07 *Performance Modeling Strategies for Modern Reinforced Concrete Bridge Columns.* Michael P. Berry and Marc O. Eberhard. April 2008.

PEER 2007/06 *Development of Improved Procedures for Seismic Design of Buried and Partially Buried Structures.* Linda Al Atik and Nicholas Sitar. June 2007.

PEER 2007/05 *Uncertainty and Correlation in Seismic Risk Assessment of Transportation Systems.* Renee G. Lee and Anne S. Kiremidjian. July 2007.

PEER 2007/04 *Numerical Models for Analysis and Performance-Based Design of Shallow Foundations Subjected to Seismic Loading.* Sivapalan Gajan, Tara C. Hutchinson, Bruce L. Kutter, Prishati Raychowdhury, José A. Ugalde, and Jonathan P. Stewart. May 2008.

PEER 2007/03 *Beam-Column Element Model Calibrated for Predicting Flexural Response Leading to Global Collapse of RC Frame Buildings.* Curt B. Haselton, Abbie B. Liel, Sarah Taylor Lange, and Gregory G. Deierlein. May 2008.

PEER 2007/02 *Campbell-Bozorgnia NGA Ground Motion Relations for the Geometric Mean Horizontal Component of Peak and Spectral Ground Motion Parameters.* Kenneth W. Campbell and Yousef Bozorgnia. May 2007.

PEER 2007/01 *Boore-Atkinson NGA Ground Motion Relations for the Geometric Mean Horizontal Component of Peak and Spectral Ground Motion Parameters.* David M. Boore and Gail M. Atkinson. May. May 2007.

PEER 2006/12 *Societal Implications of Performance-Based Earthquake Engineering.* Peter J. May. May 2007.

PEER 2006/11 *Probabilistic Seismic Demand Analysis Using Advanced Ground Motion Intensity Measures, Attenuation Relationships, and Near-Fault Effects.* Polsak Tothong and C. Allin Cornell. March 2007.

PEER 2006/10 *Application of the PEER PBEE Methodology to the I-880 Viaduct.* Sashi Kunnath. February 2007.

PEER 2006/09 *Quantifying Economic Losses from Travel Forgone Following a Large Metropolitan Earthquake.* James Moore, Sungbin Cho, Yue Yue Fan, and Stuart Werner. November 2006.

PEER 2006/08 *Vector-Valued Ground Motion Intensity Measures for Probabilistic Seismic Demand Analysis*. Jack W. Baker and C. Allin Cornell. October 2006.

PEER 2006/07 *Analytical Modeling of Reinforced Concrete Walls for Predicting Flexural and Coupled–Shear-Flexural Responses*. Kutay Orakcal, Leonardo M. Massone, and John W. Wallace. October 2006.

PEER 2006/06 *Nonlinear Analysis of a Soil-Drilled Pier System under Static and Dynamic Axial Loading.* Gang Wang and Nicholas Sitar. November 2006.

PEER 2006/05 *Advanced Seismic Assessment Guidelines.* Paolo Bazzurro, C. Allin Cornell, Charles Menun, Maziar Motahari, and Nicolas Luco. September 2006.

PEER 2006/04 *Probabilistic Seismic Evaluation of Reinforced Concrete Structural Components and Systems.* Tae Hyung Lee and Khalid M. Mosalam. August 2006.

PEER 2006/03 *Performance of Lifelines Subjected to Lateral Spreading.* Scott A. Ashford and Teerawut Juirnarongrit. July 2006.

PEER 2006/02 *Pacific Earthquake Engineering Research Center Highway Demonstration Project.* Anne Kiremidjian, James Moore, Yue Yue Fan, Nesrin Basoz, Ozgur Yazali, and Meredith Williams. April 2006.

PEER 2006/01 *Bracing Berkeley. A Guide to Seismic Safety on the UC Berkeley Campus.* Mary C. Comerio, Stephen Tobriner, and Ariane Fehrenkamp. January 2006.

PEER 2005/16 *Seismic Response and Reliability of Electrical Substation Equipment and Systems.* Junho Song, Armen Der Kiureghian, and Jerome L. Sackman. April 2006.

PEER 2005/15 *CPT-Based Probabilistic Assessment of Seismic Soil Liquefaction Initiation.* R. E. S. Moss, R. B. Seed, R. E. Kayen, J. P. Stewart, and A. Der Kiureghian. April 2006.

PEER 2005/14 *Workshop on Modeling of Nonlinear Cyclic Load-Deformation Behavior of Shallow Foundations.* Bruce L. Kutter, Geoffrey Martin, Tara Hutchinson, Chad Harden, Sivapalan Gajan, and Justin Phalen. March 2006.

PEER 2005/13 *Stochastic Characterization and Decision Bases under Time-Dependent Aftershock Risk in Performance-Based Earthquake Engineering.* Gee Liek Yeo and C. Allin Cornell. July 2005.

PEER 2005/12 *PEER Testbed Study on a Laboratory Building: Exercising Seismic Performance Assessment.* Mary C. Comerio, editor. November 2005.

PEER 2005/11 *Van Nuys Hotel Building Testbed Report: Exercising Seismic Performance Assessment.* Helmut Krawinkler, editor. October 2005.

PEER 2005/10 *First NEES/E-Defense Workshop on Collapse Simulation of Reinforced Concrete Building Structures.* September 2005.

PEER 2005/09 *Test Applications of Advanced Seismic Assessment Guidelines.* Joe Maffei, Karl Telleen, Danya Mohr, William Holmes, and Yuki Nakayama. August 2006.

PEER 2005/08 *Damage Accumulation in Lightly Confined Reinforced Concrete Bridge Columns.* R. Tyler Ranf, Jared M. Nelson, Zach Price, Marc O. Eberhard, and John F. Stanton. April 2006.

PEER 2005/07 *Experimental and Analytical Studies on the Seismic Response of Freestanding and Anchored Laboratory Equipment.* Dimitrios Konstantinidis and Nicos Makris. January 2005.

PEER 2005/06 *Global Collapse of Frame Structures under Seismic Excitations*. Luis F. Ibarra and Helmut Krawinkler. September 2005.

PEER 2005//05 *Performance Characterization of Bench- and Shelf-Mounted Equipment.* Samit Ray Chaudhuri and Tara C. Hutchinson. May 2006.

PEER 2005/04 *Numerical Modeling of the Nonlinear Cyclic Response of Shallow Foundations.* Chad Harden, Tara Hutchinson, Geoffrey R. Martin, and Bruce L. Kutter. August 2005.

PEER 2005/03 *A Taxonomy of Building Components for Performance-Based Earthquake Engineering.* Keith A. Porter. September 2005.

PEER 2005/02 *Fragility Basis for California Highway Overpass Bridge Seismic Decision Making*. Kevin R. Mackie and Božidar Stojadinović. June 2005.

PEER 2005/01 *Empirical Characterization of Site Conditions on Strong Ground Motion.* Jonathan P. Stewart, Yoojoong Choi, and Robert W. Graves. June 2005.

PEER 2004/09 *Electrical Substation Equipment Interaction: Experimental Rigid Conductor Studies.* Christopher Stearns and André Filiatrault. February 2005.

PEER 2004/08 *Seismic Qualification and Fragility Testing of Line Break 550-kV Disconnect Switches.* Shakhzod M. Takhirov, Gregory L. Fenves, and Eric Fujisaki. January 2005.

PEER 2004/07 *Ground Motions for Earthquake Simulator Qualification of Electrical Substation Equipment.* Shakhzod M. Takhirov, Gregory L. Fenves, Eric Fujisaki, and Don Clyde. January 2005.

PEER 2004/06 *Performance-Based Regulation and Regulatory Regimes.* Peter J. May and Chris Koski. September 2004.

PEER 2004/05 *Performance-Based Seismic Design Concepts and Implementation: Proceedings of an International Workshop.* Peter Fajfar and Helmut Krawinkler, editors. September 2004.

PEER 2004/04 *Seismic Performance of an Instrumented Tilt-up Wall Building.* James C. Anderson and Vitelmo V. Bertero. July 2004.

PEER 2004/03 *Evaluation and Application of Concrete Tilt-up Assessment Methodologies.* Timothy Graf and James O. Malley. October 2004.

PEER 2004/02 *Analytical Investigations of New Methods for Reducing Residual Displacements of Reinforced Concrete Bridge Columns.* Junichi Sakai and Stephen A. Mahin. August 2004.

PEER 2004/01 *Seismic Performance of Masonry Buildings and Design Implications.* Kerri Anne Taeko Tokoro, James C. Anderson, and Vitelmo V. Bertero. February 2004.

PEER 2003/18 *Performance Models for Flexural Damage in Reinforced Concrete Columns.* Michael Berry and Marc Eberhard. August 2003.

PEER 2003/17 *Predicting Earthquake Damage in Older Reinforced Concrete Beam-Column Joints.* Catherine Pagni and Laura Lowes. October 2004.

PEER 2003/16 *Seismic Demands for Performance-Based Design of Bridges.* Kevin Mackie and Božidar Stojadinović. August 2003.

PEER 2003/15 *Seismic Demands for Nondeteriorating Frame Structures and Their Dependence on Ground Motions.* Ricardo Antonio Medina and Helmut Krawinkler. May 2004.

PEER 2003/14 *Finite Element Reliability and Sensitivity Methods for Performance-Based Earthquake Engineering.* Terje Haukaas and Armen Der Kiureghian. April 2004.

PEER 2003/13 *Effects of Connection Hysteretic Degradation on the Seismic Behavior of Steel Moment-Resisting Frames.* Janise E. Rodgers and Stephen A. Mahin. March 2004.

PEER 2003/12 *Implementation Manual for the Seismic Protection of Laboratory Contents: Format and Case Studies.* William T. Holmes and Mary C. Comerio. October 2003.

PEER 2003/11 *Fifth U.S.-Japan Workshop on Performance-Based Earthquake Engineering Methodology for Reinforced Concrete Building Structures.* February 2004.

PEER 2003/10 *A Beam-Column Joint Model for Simulating the Earthquake Response of Reinforced Concrete Frames.* Laura N. Lowes, Nilanjan Mitra, and Arash Altoontash. February 2004.

PEER 2003/09 *Sequencing Repairs after an Earthquake: An Economic Approach.* Marco Casari and Simon J. Wilkie. April 2004.

PEER 2003/08 *A Technical Framework for Probability-Based Demand and Capacity Factor Design (DCFD) Seismic Formats.* Fatemeh Jalayer and C. Allin Cornell. November 2003.

PEER 2003/07 *Uncertainty Specification and Propagation for Loss Estimation Using FOSM Methods.* Jack W. Baker and C. Allin Cornell. September 2003.

PEER 2003/06 *Performance of Circular Reinforced Concrete Bridge Columns under Bidirectional Earthquake Loading*. Mahmoud M. Hachem, Stephen A. Mahin, and Jack P. Moehle. February 2003.

PEER 2003/05 *Response Assessment for Building-Specific Loss Estimation.* Eduardo Miranda and Shahram Taghavi. September 2003.

PEER 2003/04 *Experimental Assessment of Columns with Short Lap Splices Subjected to Cyclic Loads*. Murat Melek, John W. Wallace, and Joel Conte. April 2003.

PEER 2003/03 *Probabilistic Response Assessment for Building-Specific Loss Estimation.* Eduardo Miranda and Hesameddin Aslani. September 2003.

PEER 2003/02 *Software Framework for Collaborative Development of Nonlinear Dynamic Analysis Program.* Jun Peng and Kincho H. Law. September 2003.

PEER 2003/01 *Shake Table Tests and Analytical Studies on the Gravity Load Collapse of Reinforced Concrete Frames.* Kenneth John Elwood and Jack P. Moehle. November 2003.

PEER 2002/24 *Performance of Beam to Column Bridge Joints Subjected to a Large Velocity Pulse.* Natalie Gibson, André Filiatrault, and Scott A. Ashford. April 2002.

PEER 2002/23 *Effects of Large Velocity Pulses on Reinforced Concrete Bridge Columns.* Greg L. Orozco and Scott A. Ashford. April 2002.

PEER 2002/22 *Characterization of Large Velocity Pulses for Laboratory Testing.* Kenneth E. Cox and Scott A. Ashford. April 2002.

PEER 2002/21 *Fourth U.S.-Japan Workshop on Performance-Based Earthquake Engineering Methodology for Reinforced Concrete Building Structures*. December 2002.

PEER 2002/20 *Barriers to Adoption and Implementation of PBEE Innovations.* Peter J. May. August 2002.

PEER 2002/19 *Economic-Engineered Integrated Models for Earthquakes: Socioeconomic Impacts.* Peter Gordon, James E. Moore II, and Harry W. Richardson. July 2002.

PEER 2002/18 *Assessment of Reinforced Concrete Building Exterior Joints with Substandard Details.* Chris P. Pantelides, Jon Hansen, Justin Nadauld, and Lawrence D. Reaveley. May 2002.

PEER 2002/17 *Structural Characterization and Seismic Response Analysis of a Highway Overcrossing Equipped with Elastomeric Bearings and Fluid Dampers: A Case Study.* Nicos Makris and Jian Zhang. November 2002.

PEER 2002/16 *Estimation of Uncertainty in Geotechnical Properties for Performance-Based Earthquake Engineering.* Allen L. Jones, Steven L. Kramer, and Pedro Arduino. December 2002.

PEER 2002/15 *Seismic Behavior of Bridge Columns Subjected to Various Loading Patterns.* Asadollah Esmaeily-Gh. and Yan Xiao. December 2002.

PEER 2002/14 *Inelastic Seismic Response of Extended Pile Shaft Supported Bridge Structures.* T.C. Hutchinson, R.W. Boulanger, Y.H. Chai, and I.M. Idriss. December 2002.

PEER 2002/13 *Probabilistic Models and Fragility Estimates for Bridge Components and Systems.* Paolo Gardoni, Armen Der Kiureghian, and Khalid M. Mosalam. June 2002.

PEER 2002/12 *Effects of Fault Dip and Slip Rake on Near-Source Ground Motions: Why Chi-Chi Was a Relatively Mild M7.6 Earthquake.* Brad T. Aagaard, John F. Hall, and Thomas H. Heaton. December 2002.

PEER 2002/11 *Analytical and Experimental Study of Fiber-Reinforced Strip Isolators*. James M. Kelly and Shakhzod M. Takhirov. September 2002.

PEER 2002/10 *Centrifuge Modeling of Settlement and Lateral Spreading with Comparisons to Numerical Analyses***.** Sivapalan Gajan and Bruce L. Kutter. January 2003.

PEER 2002/09 *Documentation and Analysis of Field Case Histories of Seismic Compression during the 1994 Northridge, California, Earthquake.* Jonathan P. Stewart, Patrick M. Smith, Daniel H. Whang, and Jonathan D. Bray. October 2002.

PEER 2002/08 *Component Testing, Stability Analysis and Characterization of Buckling-Restrained Unbonded Braces™.* Cameron Black, Nicos Makris, and Ian Aiken. September 2002.

PEER 2002/07 *Seismic Performance of Pile-Wharf Connections.* Charles W. Roeder, Robert Graff, Jennifer Soderstrom, and Jun Han Yoo. December 2001.

PEER 2002/06 *The Use of Benefit-Cost Analysis for Evaluation of Performance-Based Earthquake Engineering Decisions*. Richard O. Zerbe and Anthony Falit-Baiamonte. September 2001.

PEER 2002/05 *Guidelines, Specifications, and Seismic Performance Characterization of Nonstructural Building Components and Equipment*. André Filiatrault, Constantin Christopoulos, and Christopher Stearns. September 2001.

PEER 2002/04 *Consortium of Organizations for Strong-Motion Observation Systems and the Pacific Earthquake Engineering Research Center Lifelines Program: Invited Workshop on Archiving and Web Dissemination of Geotechnical Data, 4–5 October 2001*. September 2002.

PEER 2002/03 *Investigation of Sensitivity of Building Loss Estimates to Major Uncertain Variables for the Van Nuys Testbed.* Keith A. Porter, James L. Beck, and Rustem V. Shaikhutdinov. August 2002.

PEER 2002/02 *The Third U.S.-Japan Workshop on Performance-Based Earthquake Engineering Methodology for Reinforced Concrete Building Structures*. July 2002.

PEER 2002/01 *Nonstructural Loss Estimation: The UC Berkeley Case Study.* Mary C. Comerio and John C. Stallmeyer. December 2001.

PEER 2001/16 *Statistics of SDF-System Estimate of Roof Displacement for Pushover Analysis of Buildings.* Anil K. Chopra, Rakesh K. Goel, and Chatpan Chintanapakdee. December 2001.

PEER 2001/15 *Damage to Bridges during the 2001 Nisqually Earthquake.* R. Tyler Ranf, Marc O. Eberhard, and Michael P. Berry. November 2001.

PEER 2001/14 *Rocking Response of Equipment Anchored to a Base Foundation.* Nicos Makris and Cameron J. Black. September 2001.

PEER 2001/13 *Modeling Soil Liquefaction Hazards for Performance-Based Earthquake Engineering.* Steven L. Kramer and Ahmed-W. Elgamal. February 2001.

PEER 2001/12 *Development of Geotechnical Capabilities in OpenSees.* Boris Jeremi . September 2001.

PEER 2001/11 *Analytical and Experimental Study of Fiber-Reinforced Elastomeric Isolators*. James M. Kelly and Shakhzod M. Takhirov. September 2001.

PEER 2001/10 *Amplification Factors for Spectral Acceleration in Active Regions.* Jonathan P. Stewart, Andrew H. Liu, Yoojoong Choi, and Mehmet B. Baturay. December 2001.

PEER 2001/09 *Ground Motion Evaluation Procedures for Performance-Based Design.* Jonathan P. Stewart, Shyh-Jeng Chiou, Jonathan D. Bray, Robert W. Graves, Paul G. Somerville, and Norman A. Abrahamson. September 2001.

PEER 2001/08 *Experimental and Computational Evaluation of Reinforced Concrete Bridge Beam-Column Connections for Seismic Performance*. Clay J. Naito, Jack P. Moehle, and Khalid M. Mosalam. November 2001.

PEER 2001/07 *The Rocking Spectrum and the Shortcomings of Design Guidelines.* Nicos Makris and Dimitrios Konstantinidis. August 2001.

PEER 2001/06 *Development of an Electrical Substation Equipment Performance Database for Evaluation of Equipment Fragilities*. Thalia Agnanos. April 1999.

PEER 2001/05 *Stiffness Analysis of Fiber-Reinforced Elastomeric Isolators.* Hsiang-Chuan Tsai and James M. Kelly. May 2001.

PEER 2001/04 *Organizational and Societal Considerations for Performance-Based Earthquake Engineering.* Peter J. May. April 2001.

PEER 2001/03 *A Modal Pushover Analysis Procedure to Estimate Seismic Demands for Buildings: Theory and Preliminary Evaluation.* Anil K. Chopra and Rakesh K. Goel. January 2001.

PEER 2001/02 *Seismic Response Analysis of Highway Overcrossings Including Soil-Structure Interaction.* Jian Zhang and Nicos Makris. March 2001.

PEER 2001/01 *Experimental Study of Large Seismic Steel Beam-to-Column Connections.* Egor P. Popov and Shakhzod M. Takhirov. November 2000.

PEER 2000/10 *The Second U.S.-Japan Workshop on Performance-Based Earthquake Engineering Methodology for Reinforced Concrete Building Structures.* March 2000.

PEER 2000/09 *Structural Engineering Reconnaissance of the August 17, 1999 Earthquake: Kocaeli (Izmit), Turkey.* Halil Sezen, Kenneth J. Elwood, Andrew S. Whittaker, Khalid Mosalam, John J. Wallace, and John F. Stanton. December 2000.

PEER 2000/08 *Behavior of Reinforced Concrete Bridge Columns Having Varying Aspect Ratios and Varying Lengths of Confinement.* Anthony J. Calderone, Dawn E. Lehman, and Jack P. Moehle. January 2001.

PEER 2000/07 *Cover-Plate and Flange-Plate Reinforced Steel Moment-Resisting Connections*. Taejin Kim, Andrew S. Whittaker, Amir S. Gilani, Vitelmo V. Bertero, and Shakhzod M. Takhirov. September 2000.

PEER 2000/06 *Seismic Evaluation and Analysis of 230-kV Disconnect Switches.* Amir S. J. Gilani, Andrew S. Whittaker, Gregory L. Fenves, Chun-Hao Chen, Henry Ho, and Eric Fujisaki. July 2000.

PEER 2000/05 *Performance-Based Evaluation of Exterior Reinforced Concrete Building Joints for Seismic Excitation.* Chandra Clyde, Chris P. Pantelides, and Lawrence D. Reaveley. July 2000.

PEER 2000/04 *An Evaluation of Seismic Energy Demand: An Attenuation Approach.* Chung-Che Chou and Chia-Ming Uang. July 1999.

PEER 2000/03 *Framing Earthquake Retrofitting Decisions: The Case of Hillside Homes in Los Angeles.* Detlof von Winterfeldt, Nels Roselund, and Alicia Kitsuse. March 2000.

PEER 2000/02 *U.S.-Japan Workshop on the Effects of Near-Field Earthquake Shaking.* Andrew Whittaker, ed. July 2000.

PEER 2000/01 *Further Studies on Seismic Interaction in Interconnected Electrical Substation Equipment.* Armen Der Kiureghian, Kee-Jeung Hong, and Jerome L. Sackman. November 1999.

PEER 1999/14 *Seismic Evaluation and Retrofit of 230-kV Porcelain Transformer Bushings*. Amir S. Gilani, Andrew S. Whittaker, Gregory L. Fenves, and Eric Fujisaki. December 1999.

PEER 1999/13 *Building Vulnerability Studies: Modeling and Evaluation of Tilt-up and Steel Reinforced Concrete Buildings.* John W. Wallace, Jonathan P. Stewart, and Andrew S. Whittaker, editors. December 1999.

PEER 1999/12 *Rehabilitation of Nonductile RC Frame Building Using Encasement Plates and Energy-Dissipating Devices.* Mehrdad Sasani, Vitelmo V. Bertero, James C. Anderson. December 1999.

PEER 1999/11 *Performance Evaluation Database for Concrete Bridge Components and Systems under Simulated Seismic Loads.* Yael D. Hose and Frieder Seible. November 1999.

PEER 1999/10 *U.S.-Japan Workshop on Performance-Based Earthquake Engineering Methodology for Reinforced Concrete Building Structures.* December 1999.

PEER 1999/09 *Performance Improvement of Long Period Building Structures Subjected to Severe Pulse-Type Ground Motions*. James C. Anderson, Vitelmo V. Bertero, and Raul Bertero. October 1999.

PEER 1999/08 *Envelopes for Seismic Response Vectors.* Charles Menun and Armen Der Kiureghian. July 1999.

PEER 1999/07 *Documentation of Strengths and Weaknesses of Current Computer Analysis Methods for Seismic Performance of Reinforced Concrete Members.* William F. Cofer. November 1999.

PEER 1999/06 *Rocking Response and Overturning of Anchored Equipment under Seismic Excitations.* Nicos Makris and Jian Zhang. November 1999.

PEER 1999/05 *Seismic Evaluation of 550 kV Porcelain Transformer Bushings.* Amir S. Gilani, Andrew S. Whittaker, Gregory L. Fenves, and Eric Fujisaki. October 1999.

PEER 1999/04 *Adoption and Enforcement of Earthquake Risk-Reduction Measures.* Peter J. May, Raymond J. Burby, T. Jens Feeley, and Robert Wood.

PEER 1999/03 *Task 3 Characterization of Site Response General Site Categories*. Adrian Rodriguez-Marek, Jonathan D. Bray, and Norman Abrahamson. February 1999.

PEER 1999/02 *Capacity-Demand-Diagram Methods for Estimating Seismic Deformation of Inelastic Structures: SDF Systems*. Anil K. Chopra and Rakesh Goel. April 1999.

PEER 1999/01 *Interaction in Interconnected Electrical Substation Equipment Subjected to Earthquake Ground Motions.* Armen Der Kiureghian, Jerome L. Sackman, and Kee-Jeung Hong. February 1999.

PEER 1998/08 *Behavior and Failure Analysis of a Multiple-Frame Highway Bridge in the 1994 Northridge Earthquake.* Gregory L. Fenves and Michael Ellery. December 1998.

PEER 1998/07 *Empirical Evaluation of Inertial Soil-Structure Interaction Effects.* Jonathan P. Stewart, Raymond B. Seed, and Gregory L. Fenves. November 1998.

PEER 1998/06 *Effect of Damping Mechanisms on the Response of Seismic Isolated Structures.* Nicos Makris and Shih-Po Chang. November 1998.

PEER 1998/05 *Rocking Response and Overturning of Equipment under Horizontal Pulse-Type Motions.* Nicos Makris and Yiannis Roussos. October 1998.

PEER 1998/04 *Pacific Earthquake Engineering Research Invitational Workshop Proceedings, May 14–15, 1998: Defining the Links between Planning, Policy Analysis, Economics and Earthquake Engineering.* Mary Comerio and Peter Gordon. September 1998.

PEER 1998/03 *Repair/Upgrade Procedures for Welded Beam to Column Connections.* James C. Anderson and Xiaojing Duan. May 1998.

PEER 1998/02 *Seismic Evaluation of 196 kV Porcelain Transformer Bushings.* Amir S. Gilani, Juan W. Chavez, Gregory L. Fenves, and Andrew S. Whittaker. May 1998.

PEER 1998/01 *Seismic Performance of Well-Confined Concrete Bridge Columns.* Dawn E. Lehman and Jack P. Moehle. December 2000.

ONLINE REPORTS

The following PEER reports are available by Internet only at http://peer.berkeley.edu/publications/peer_reports.html

PEER 2010/101 *Rocking Response of Bridges on Shallow Foundations.* José A. Ugalde, Bruce L. Kutter, and Boris Jeremić. April 2010.

PEER 2009/109 *Simulation and Performance-Based Earthquake Engineering Assessment of Self-Centering Post-Tensioned Concrete Bridge Systems.* Won K. Lee and Sarah L. Billington. December 2009.

PEER 2009/108 *PEER Lifelines Geotechnical Virtual Data Center.* J. Carl Stepp, Daniel J. Ponti, Loren L. Turner, Jennifer N. Swift, Sean Devlin, Yang Zhu, Jean Benoit, and John Bobbitt. September 2009.

PEER 2009/107 *Experimental and Computational Evaluation of Current and Innovative In-Span Hinge Details in Reinforced Concrete Box-Girder Bridges: Part 2: Post-Test Analysis and Design Recommendations.* Matias A. Hube and Khalid M. Mosalam. December 2009.

PEER 2009/106 *Shear Strength Models of Exterior Beam-Column Joints without Transverse Reinforcement.* Sangjoon Park and Khalid M. Mosalam. November 2009.

PEER 2009/105 *Reduced Uncertainty of Ground Motion Prediction Equations through Bayesian Variance Analysis.* Robb Eric S. Moss. November 2009.

PEER 2009/104 *Advanced Implementation of Hybrid Simulation.* Andreas H. Schellenberg, Stephen A. Mahin, Gregory L. Fenves. November 2009.

PEER 2009/103 *Performance Evaluation of Innovative Steel Braced Frames.* T. Y. Yang, Jack P. Moehle, and Božidar Stojadinovic. August 2009.

PEER 2009/102 *Reinvestigation of Liquefaction and Nonliquefaction Case Histories from the 1976 Tangshan Earthquake.* Robb Eric Moss, Robert E. Kayen, Liyuan Tong, Songyu Liu, Guojun Cai, and Jiaer Wu. August 2009.

PEER 2009/101 *Report of the First Joint Planning Meeting for the Second Phase of NEES/E-Defense Collaborative Research on Earthquake Engineering.* Stephen A. Mahin et al. July 2009.

PEER 2008/104 *Experimental and Analytical Study of the Seismic Performance of Retaining Structures.* Linda Al Atik and Nicholas Sitar. January 2009.

PEER 2008/103 *Experimental and Computational Evaluation of Current and Innovative In-Span Hinge Details in Reinforced Concrete Box-Girder Bridges. Part 1: Experimental Findings and Pre-Test Analysis.* Matias A. Hube and Khalid M. Mosalam. January 2009.

PEER 2008/102 *Modeling of Unreinforced Masonry Infill Walls Considering In-Plane and Out-of-Plane Interaction.* Stephen Kadysiewski and Khalid M. Mosalam. January 2009.

PEER 2008/101 *Seismic Performance Objectives for Tall Buildings.* William T. Holmes, Charles Kircher, William Petak, and Nabih Youssef. August 2008.

PEER 2007/101 *Generalized Hybrid Simulation Framework for Structural Systems Subjected to Seismic Loading.* Tarek Elkhoraibi and Khalid M. Mosalam. July 2007.

PEER 2007/100 *Seismic Evaluation of Reinforced Concrete Buildings Including Effects of Masonry Infill Walls.* Alidad Hashemi and Khalid M. Mosalam. July 2007.